CHAPTER

Electrodynamic loudspeakers

6

CHAPTER OUTLINE

PART XIX: BASIC THEORY OF ELECTRODYNAMIC LOUDSPEAKERS

6.1 INTRODUCTION

An electrodynamic or moving-coil loudspeaker is an electromagnetic transducer for converting electrical signals into sounds. When the original version of this book was published in 1954 under the title *Acoustics*, the only practical amplifying device available was the vacuum tube, so output power was expensive. Hence the efficiency of the electrodynamic loudspeaker was one of the most important factors. As the cost of amplifier watts has decreased, there has been a steady trend towards smaller loudspeakers coupled with ever more powerful amplifiers, which are needed to compensate for the reduced radiating efficiency of the smaller diaphragms. Two developments have spurred this trend: the replacement of the vacuum tube with silicon transistor and the introduction of so-called digital amplifiers using various coding schemes, the most popular being pulse-width modulation or Class D.

Acoustics: Sound Fields and Transducers. DOI: 10.1016/B978-0-12-391421-7.00006-3

In mobile devices, which rely on battery power, the efficiency issue has not gone away. The most important development for mobile devices has been the introduction of rare-earth neodymium magnets, which have enabled significant miniaturization. One trend which has enabled loudspeakers of all sizes to be used with smaller enclosures has been the development of high-compliance suspensions which are stable enough not to cause rocking modes. The term "acoustic suspension" has been dubbed [1] to describe a loudspeaker which has an enclosure so small that the air inside the enclosure is stiffer than the suspension.

There are two principal types of loudspeakers: those in which the vibrating surface (called the diaphragm) radiates sound directly into the air, and those in which a horn is interposed between the diaphragm and the air. The direct-radiator type is used in most home and car entertainment, mobile devices, and in small public-address systems. The horn type is used in more exotic hi-fi systems (especially those using tubes), in large sound systems in theaters and auditoriums, and in music and outdoor-announcing systems.

The principal advantages of the direct-radiator type are (1) small size, (2) low cost, and (3) a satisfactory response over a comparatively wide frequency range. The principal disadvantages are (1) low efficiency, (2) narrow directivity pattern at high frequencies. For use in home, car, and mobile audio, where little acoustic power is necessary, the advantages far outweigh the disadvantages. In theater and outdoor sound systems where large amounts of acoustic power are necessary and where space is not important, the more efficient horn-type loudspeaker is generally used.

All the types of transduction discussed in the previous chapter on Microphones might be used for loudspeakers. In this text, however, we shall limit ourselves to electrodynamic loudspeakers, the type most commonly used in home, car, mobile, and professional audio.

6.2 CONSTRUCTION [2]

A cross-sectional sketch of a typical loudspeaker drive unit is shown in Fig. 6.1. The diaphragm (1) is a cone made from a suitably light and stiff material, although most of the stiffness comes from the fact that it is curved. In the center is a dust cap (2) which guards against metallic dust fouling the magnetic gap and prevents sound from the back of the diaphragm leaking through to the outside world. If the loudspeaker were mounted in a bass-reflex enclosure, such leakage could seriously reduce the Q of the port resonance. Attached to the top of the cone is a coil former upon which the coil (3) is wound. This coil is located in the gap of a magnetic path, comprising a pole piece (4) and pole plate (5), where the magnetic flux is produced by a permanent magnet (6), which is held in place by a basket structure (7). The diaphragm is supported at the rim and near the voice coil by a surround (8) and spider (9), respectively, so that it is free to move only in an axial direction. The name "spider" originates from the early electrodynamic loudspeakers in which the cone was supported by a spider-like slotted disk that was anchored to the pole-piece in place of the dust cap. Apart from this modification and the switch from electromagnets to alnico (Aluminum-Nickel-Cobalt) permanent magnets in the 1930s and then to ferrite magnets in the 1970s (for economic reasons, not performance related), there has been very little change in the construction of electrodynamic loudspeakers since the Rice–Kellogg [3] patent of 1924. We will refer to the spider and surround as the suspension. In general, sound from the back of the cone exits through holes in the basket (7), while sound from the back of the dome (2) leaks through the magnetic gap and spider (9), which is often made from a phenolic-resin impregnated textile, before exiting through the basket.

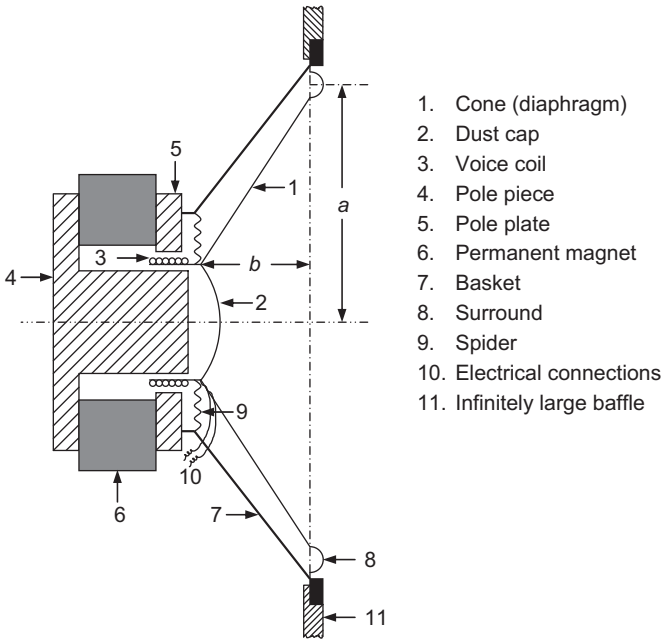

FIG. 6.1 Cross-sectional sketch of a direct-radiator loudspeaker assumed to be mounted in an infinite baffle.

When an audio signal is applied to the electrical connections (10), the resulting current through the voice coil creates a magnetomotive force which interacts with the air-gap flux of the permanent magnet and causes a translatory movement of the voice coil and, hence, of the cone to which it is attached. The movement of the cone in turn displaces the air molecules at its surface thus producing sound waves. Usually the cone is sufficiently stiff at low frequencies to move as a whole. At high frequencies, however, vibrations from the center travel outward toward the edge in the form of waves. The results of these traveling waves and of resonances in the cone itself are to produce irregularities in the frequency-response curve at the higher frequencies and to influence the relative amounts of sound radiated in different directions. Unless treated, Metal cones have relatively low internal damping and tend to produce high Q resonances, but at higher frequencies than paper or polymer cones due to their high ratio of flexural rigidity to density. Care needs to be taken in the choice of surround material and means of attachment to the coil former in order to minimize such resonances. Paper and polymer cones have greater damping so that the compression waves propagating through the cone from the coil are mainly absorbed at higher frequencies. This leads to an interesting phenomenon whereby the effective radiating area of the cone decreases with frequency, which is beneficial for maintaining a widely dispersed sound field. Eventually, only the dust cap radiates and the stationary cone acts as a horn. We will discuss the vibration modes of the cone later in this chapter.

In Fig. 6.1, the drive unit is shown mounted in a flat baffle (11) assumed to be of infinite extent. Obviously this is not possible in practice, but it is an ideal configuration which simplifies our

analysis of the drive unit. By definition, a baffle is any means for acoustically isolating the front side of the diaphragm from the rear side. For purposes of analysis, the diaphragm may be considered at low frequencies to be a planar piston of radius a moving with uniform velocity over its entire surface. This is a fair approximation at frequencies for which the distance b on Fig. 6.1 is less than about one-tenth wavelength. The piston in an infinite baffle is the only sound source which gives a uniformly flat far-field on-axis response under constant acceleration, and this phenomenon is explained in Sec. 6.6.

6.3 ELECTRO-MECHANO-ACOUSTICAL CIRCUIT

Before drawing a circuit diagram for a loudspeaker, we must identify the various elements involved. The voice coil has inductance and resistance, which we shall call L_E and R_E, respectively. The diaphragm and the wire on the voice coil have a total mass M_{MD}. The diaphragm is mounted on flexible suspensions at the center and at the edge. The total effect of these suspensions may be represented by a mechanical compliance C_{MS} and a mechanical resistance $R_{MS} = 1/G_{MS}$, where G_{MS} is the mechanical conductance. The air cavity and the holes at the rear of the center portion of the diaphragm form an acoustic network which, in most loudspeakers, can be neglected in analysis because they have no appreciable influence on the performance of the loudspeaker. However, both the rear and the front side of the main part of the diaphragm radiate sound into the open air.

An acoustic radiation impedance is assigned to each side and is designated as $Z_{AR} = 1/Y_{AR}$, where Y_{AR} is the acoustic radiation admittance. Thus the mechanical radiation admittance seen by each side of the diaphragm is $Y_{MR} = S_D^2 Y_{AR}$, where S_D is the effective diaphragm area. Approximate equivalent circuits for Y_{MR} and Y_{AR} are given in Fig. 4.37c and d respectively.

We observe that one side of each flexible suspension is at zero velocity. For the mechanical resistance this also must be true because it is contained in the suspensions. We already know from earlier chapters that one side of the mass and one side of the radiation admittance must be considered as having zero velocity. Similarly, we note that the other sides of the masses, the compliance, the conductance, and the radiation admittances all have the same velocity, viz., that of the voice coil.

From inspection we are able to draw a mechanical circuit and the electromechanical analogous circuit using the admittance analogy. These are shown in Fig. 6.2a and b, respectively. The symbols have the following meanings:

$\tilde{e}_g$ is open-circuit voltage of the generator (audio amplifier) in volts (V).
R_g is generator resistance in electrical ohms (Ω).
L_E is inductance of voice coil in henrys (H), measured with the voice-coil movement blocked, i.e., for $\tilde{u}_c = 0$.
R_E is resistance of voice coil in electrical ohms (Ω), measured in the same manner as L_E
B is steady air-gap magnetic field or flux density in Tesla (T).
l is length of wire in m on the voice-coil winding.
$\tilde{i}$ is electric current in amperes (A) through the voice-coil winding.
$\tilde{f}_c$ is force in N generated by interaction between the alternating and steady mmfs, that is, $\tilde{f}_c = Bl\tilde{i}$.
$\tilde{u}_c$ is voice-coil velocity in m/s, that is, $\tilde{u}_c = \tilde{e}/Bl$, where $\tilde{e}$ is the so-called counter emf.

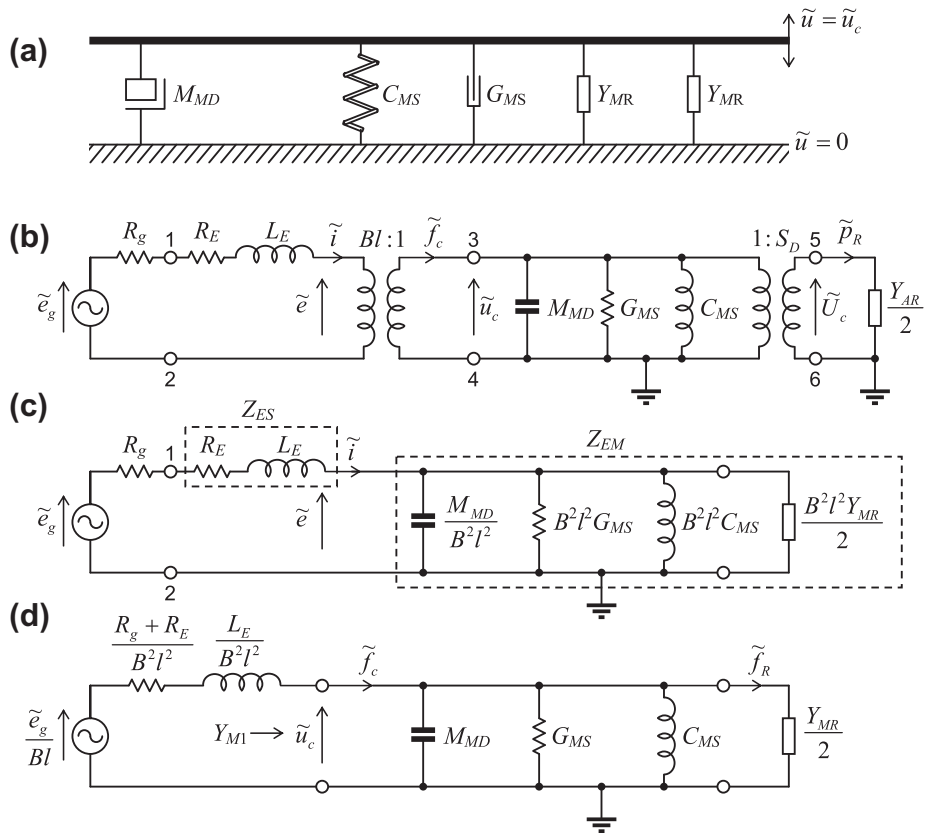

FIG. 6.2 (a) Mechanical circuit of direct-radiator loudspeaker; (b) electro-mechano-acoustical analogous circuit of the admittance type; (c) electrical circuit showing static electrical impedance Z_{ES} and motional electrical impedance Z_{EM}; (d) analogous circuit of the admittance type with electrical quantities referred to the mechanical side.

a is radius of diaphragm in m.
M_{MD} is mass of the diaphragm and the voice coil in kg.
C_{MS} is total mechanical compliance of the suspensions in m/N.
$G_{MS} = 1/R_{MS}$ is mechanical conductance of the suspension in $\mathrm{m \cdot N^{-1} \cdot s^{-1}}$.
R_{MS} is mechanical resistance of the suspensions in $\mathrm{N \cdot s/m}$.
$Y_{MR} = 1/Z_{MR} = \boldsymbol{G}_{MR} + jB_{MR}$ is mechanical radiation admittance in $\mathrm{m \cdot N^{-1} \cdot s^{-1}}$ from one side of the diaphragm (see Fig. 4.36). The bold $\boldsymbol{G}$ indicates that $\boldsymbol{G}_{MR}$ varies with frequency.
$Z_{MR} = \boldsymbol{R}_{MR} + jX_{MR}$ is mechanical radiation impedance in $\mathrm{N \cdot s/m}$ from one side of a piston of radius a mounted in an infinite baffle (see Fig. 4.35). The bold $\boldsymbol{R}$ indicates that $\boldsymbol{R}_{MS}$ varies with frequency.
$S_D = \pi a^2$ is effective area of diaphragm in $\mathrm{m^2}$.
$\tilde{p}_R$ is pressure on the diaphragm due to the radiation load, that is, $\tilde{p}_R = 2\tilde{U}_c/Y_{MR}$.
$\tilde{U}_c$ is volume velocity produced by the diaphragm, that is, $\tilde{U}_c = S_D\tilde{u}_c$.

It should be noted that the coil inductance L_E is highly nonlinear. In practice, the reactive coil impedance does not rise linearly with frequency but is roughly proportional to the square-root of frequency. A more accurate model [4] can be made by adding a second inductor with a resistor in parallel with it, but in this text we shall use the simple model with a single inductor.

The circuit of Fig. 6.2b with the mechanical side brought through the transformer to the electrical side is shown in Fig. 6.2c. Hence this represents the circuit as seen from the input terminals. It is important for several reasons. Firstly, we have to take the electrical impedance into account when considering the load presented by the loudspeaker to the amplifier driving it. The loading effect will also modify the frequency response of any passive crossover network that may be used. Also, we can calculate the parameters of a drive unit by measuring the input impedance, as will be explained in Sec. 6.10, without the need for an anechoic chamber. The mechanical admittance $Y_{M1} = \tilde{u}_c/\tilde{f}_c$ is zero if the diaphragm is blocked so that there is no motion $(\tilde{u}_c = 0)$ but has a value different from zero whenever there is motion. For this reason the quantity $Z_{EM} = B^2l^2Y_{M1}$ is usually called the motional electrical impedance. A quantity often found on data sheets is the electrical suspension resistance $R_{ES} = B^2l^2G_{MS} = B^2l^2/R_{MS}$. This resistance is in series with the coil resistance R_E at resonance. When the electrical side is brought over to the mechanical side, we have the circuit of Fig. 6.2d.

The circuit of Fig. 6.2d will be easier to solve if its form is modified. First we recognize the equivalence of the two circuits shown in Fig. 6.3a and b according to *Norton's theorem* (see Fig. 14.4). Next we substitute Fig. 6.3b for its equivalent in Fig. 6.2d. Then we take the dual of Fig. 6.2d to obtain Fig. 6.4a. (See Fig. 3.41 and Fig. 3.42).

The performance of a direct-radiator loudspeaker is directly related to the diaphragm velocity. Having solved for it, we may compute the acoustic power radiated and the sound pressure produced at any given distance from the loudspeaker in the far-field.

Voice-coil velocity at medium and low frequencies. The voice-coil velocity $\tilde{u}_c$, neglecting ω^2L^2 compared with $(R_g + R_E)^2$, is found from Fig. 6.4a,

$$\tilde{u}_c \approx \frac{\tilde{e}_g Bl}{(R_g + R_E)(R_M + jX_M)} \tag{6.1}$$

where

$$R_M = \frac{B^2l^2}{R_g + R_E} + R_{MS} + 2\boldsymbol{R}_{MR} \tag{6.2}$$

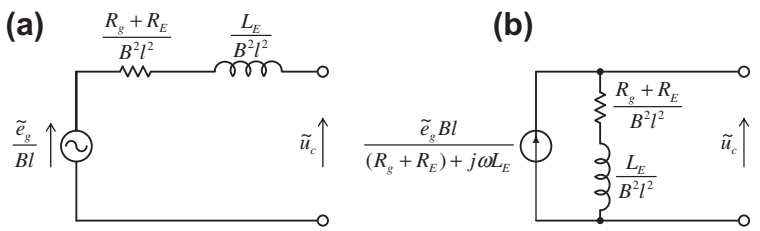

FIG. 6.3 The electrical circuit (referred to the mechanical side) is shown here in two equivalent forms according to Norton's theorem.

The circuits are of the admittance type. (Note: The generator in (b) is of constant flow type.)

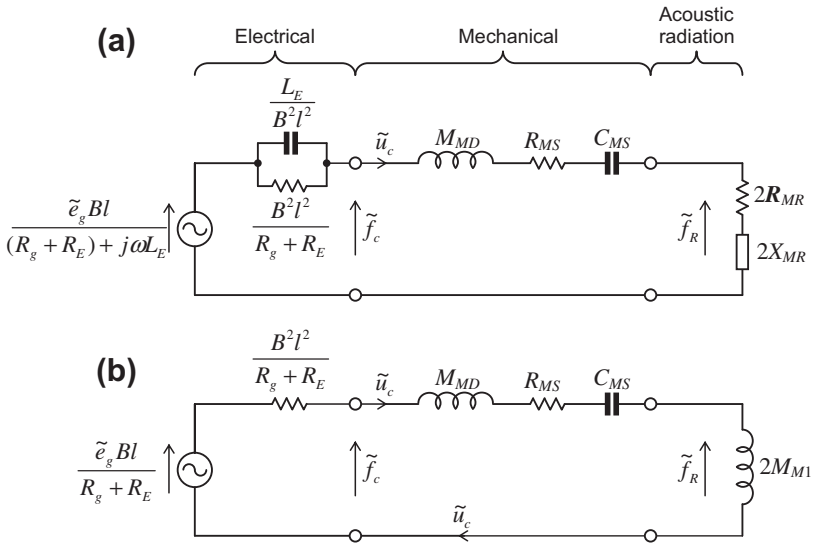

FIG. 6.4 (a) Low-frequency analogous circuit of the impedance type with electrical quantities referred to mechanical side.

Z_{MR} is given by Fig. 4.35. The quantity $\tilde{f}_c$ represents the total force acting in the equivalent circuit to produce the voice-coil velocity $\tilde{u}_c$. (b) Single-loop approximation to Fig. 6.4a valid for $X_{MR}{}^2 >> \boldsymbol{R}_{MR}{}^2$.

$$X_M = \omega M_M = \omega M_{MD} + 2X_{MR} - \frac{1}{\omega C_{MS}} \tag{6.3}$$

Voice-coil velocity at low frequencies. At low frequencies, assuming in addition that $X_{MR}^2 >> \boldsymbol{R}_{MR}^2$ we have from Fig. 6.4b that

$$(X_M)_{\text{low } f} = \omega(M_{MD} + 2M_{M1}) - \frac{1}{\omega C_{MS}} \tag{6.4}$$

where

$$M_{M1} = 2.67a^3\rho_0 \tag{6.5}$$

is the mass in kg contributed by the air load on one side of the piston for the frequency range in which $ka < 0.5$. (See Table 4.4). The quantity ka equals the ratio of the circumference of the diaphragm to the wavelength.

The voice-coil velocity is found from Eq. (6.1), using Eqs. (6.2) and (6.4) for R_M and X_M, respectively so that

$$\tilde{u}_c = \frac{\tilde{e}_g}{BlQ_{ES}}\beta_c(f) \tag{6.6}$$

where $\beta_c(f)$ is a dimensionless frequency response function given by

$$\beta_c(f) = \frac{j\dfrac{f}{f_S}}{1-\dfrac{f^2}{f_S^2}+j\dfrac{1}{Q_{TS}}.\dfrac{f}{f_S}} \tag{6.7}$$

The suspension resonance frequency f_S is given by

$$f_S = \frac{1}{2\pi\sqrt{M_{MS}C_{MS}}}, \tag{6.8}$$

where $M_{MS} = M_{MD} + 2M_{M1}$ is the combined diaphragm and air-load mass, and

$$Q_{TS} = \left(\frac{B^2l^2}{R_g + R_E} + R_{MS}\right)^{-1}\sqrt{\frac{M_{MS}}{C_{MS}}}. \tag{6.9}$$

When $f = f_S$, the real terms in the denominator of Eq. (6.7) vanish and we see from Eq. (6.9) that the total Q value of the suspension resonance equals Q_{TS} where Q_{TS} is the reciprocal of the effective resistance in the mechanical circuit multiplied by the square root of the ratio of the mass to the compliance of the diaphragm. If we define f_1 and f_2 as the frequencies at which the velocity is 3 dB below its peak value, then $Q_{TS} = f_S/(f_2 - f_1)$. Therefore increasing the Q value increases the height of the resonance peak while decreasing its width. At f_S, the inertial and static reactances in Fig. 6.4b cancel each other so that the velocity $\tilde{u}_c$ is simply the driving force (first term in Eq. (6.6)) divided by the total resistance in the loop, as shown in Fig. 6.6b. The total Q can be separated into two parts

$$Q_{TS} = \frac{1}{\dfrac{1}{Q_{ES}} + \dfrac{1}{Q_{MS}}} = \frac{Q_{ES}Q_{MS}}{Q_{ES} + Q_{MS}} \tag{6.10}$$

namely the electrical Q

$$Q_{ES} = \frac{R_g + R_E}{B^2l^2}\sqrt{\frac{M_{MS}}{C_{MS}}} \tag{6.11}$$

and the mechanical Q

$$Q_{MS} = \frac{1}{R_{MS}}\sqrt{\frac{M_{MS}}{C_{MS}}} \tag{6.12}$$

The normalized velocity is plotted in Fig. 6.5 using $20\log_{10}|\beta_c|$. It is a universal resonance curve. Below the resonance frequency it has a slope of +6 dB per octave of frequency. Above the resonance frequency it has a slope of −6 dB per octave. The acceleration is given by the first time derivative of the velocity

$$\tilde{a}_c = j\omega\tilde{u}_c = \frac{2\pi f_S\tilde{e}_g}{BlQ_{ES}}\alpha_c(f) \tag{6.13}$$

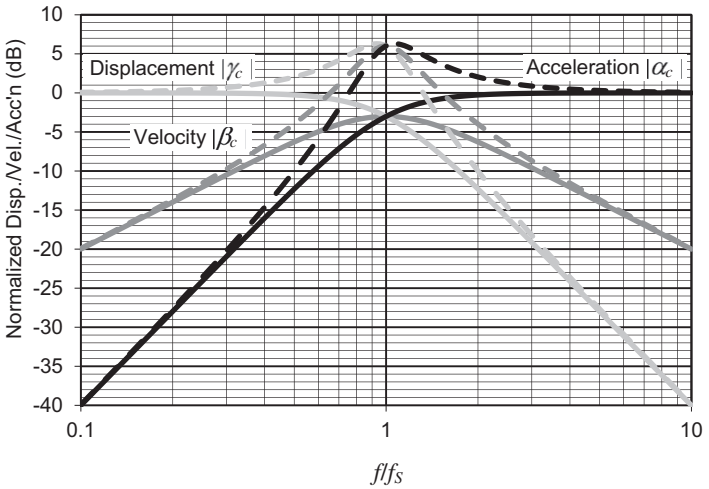

FIG. 6.5 Normalized voice-coil displacement, velocity, and acceleration.

The solid line is for $Q_{TS} = 1/\sqrt{2}$. The dashed line is for $Q_{TS} = 2$.

where $\alpha_c(f)$ is a dimensionless frequency response function given by

$$\alpha_c(f) = \frac{-\dfrac{f^2}{f_S^2}}{1 - \dfrac{f^2}{f_S^2} + j\dfrac{1}{Q_{TS}} \cdot \dfrac{f}{f_S}} \tag{6.14}$$

The displacement is given by the first time integral of the velocity

$$\tilde{\eta}_c = \frac{\tilde{u}_c}{j\omega} = \frac{\tilde{e}_g}{2\pi f_S Bl Q_{ES}} \gamma_c(f) \tag{6.15}$$

where $\gamma_c(f)$ is a dimensionless frequency response function given by

$$\gamma_c(f) = \frac{1}{1 - \dfrac{f^2}{f_S^2} + j\dfrac{1}{Q_{TS}} \cdot \dfrac{f}{f_S}} \tag{6.16}$$

The normalized displacement and acceleration are also plotted in Fig. 6.5 along with the velocity. We see that when $f/f_S \leq 1/3$, the displacement is virtually constant. This is the *stiffness-controlled* range in which the displacement is simply the static deflection as determined by Hooke's law, that is, the product of the driving force and the compliance:

$$\tilde{\eta}_c\Big|_{f \leq 1/3\, f_s} \approx \frac{\tilde{e}_g Bl}{R_g + R_E} C_{MS} \tag{6.17}$$

The displacement curve is that of a second-order low-pass filter with a 12 dB/octave slope when $f/f_S \geq 3$. As is seen from Eq. (6.16), the displacement in this range is proportional to $1/f^2$ and the equivalent

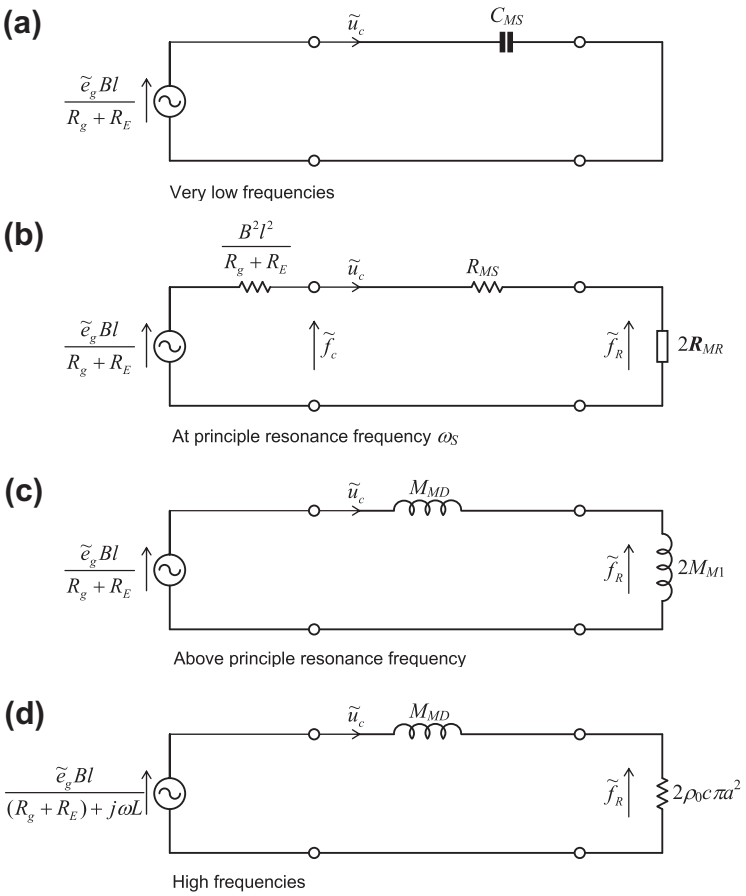

FIG. 6.6 Simplified forms of the circuit of Fig. 6.4a valid over limited frequency ranges.

circuit is that shown in Fig. 6.6a. When $f/f_S \geq 3$, the acceleration is virtually constant. This is the *mass-controlled* range in which the acceleration is simply the driving force divided by the mass in accordance with Newton's second law of motion

$$\tilde{a}_c\big|_{f \leq 3\, f_s} \approx \frac{\tilde{e}_g Bl}{(R_g + R_E) M_{MS}} \tag{6.18}$$

The acceleration curve is that of a second-order high-pass filter with a 12 dB/octave slope when $f/f_S \leq 1/3$. As can be seen from Eq. (6.16), the acceleration in this range is proportional to f^2 and the equivalent circuit is that shown in Fig. 6.6c.

6.4 POWER OUTPUT

The acoustic power radiated in watts from both the rear and the front sides of the loudspeaker is

$$W = \left|\frac{\tilde{u}_c}{\sqrt{2}}\right|^2 (2\boldsymbol{R}_{MR}) \tag{6.19}$$

Hence, assuming $\omega^2 L^2 << (R_g + R_E)^2$, and using Eq. (6.1) for $\tilde{u}_c$ we obtain

$$W = \left|\frac{\tilde{e}_g}{\sqrt{2}}\right|^2 \frac{2B^2 l^2 \boldsymbol{R}_{MR}}{(R_g + R_E)^2 (R_M^2 + X_M^2)} \tag{6.20}$$

Above the suspension resonance frequency, the diaphragm mass dominates so that $X_M >> R_M$ where $X_M \approx j\omega M_{MS}$. Also, when the wavelength is small compared with the diameter of the diaphragm, we see from Table 4.4 that

$$\boldsymbol{R}_{MR} = \frac{\omega^2 S_D^2 \rho_0}{2\pi c} \tag{6.21}$$

where

$$S_D = \pi a^2 \tag{6.22}$$

is the *effective* area of the diaphragm of Fig. 6.1. Inserting these into Eq. (6.20) yields

$$W = \frac{e_{g(\text{rms})}^2 B^2 l^2 S_D^2 \rho_0}{\pi (R_g + R_E)^2 M_{MS}^2 c}, \qquad 2f_0 < f < \frac{c}{4\pi a} \tag{6.23}$$

where

$$e_{g(\text{rms})} = \left|\frac{\tilde{e}_g}{\sqrt{2}}\right| \tag{6.24}$$

In this frequency range, the radiated power is fairly constant because, as the frequency increases, the falling velocity is compensated for by the rising radiation resistance. At higher frequencies where $\boldsymbol{R}_{MR} = S_D \rho_0 c$, we have

$$W = \frac{2e_{g(\text{rms})}^2 B^2 l^2 S_D \rho_0 c}{(R_g + R_E)^2 \omega^2 M_{MS}^2}, \qquad f > \frac{5c}{2\pi a} \tag{6.25}$$

Hence the radiated power is proportional to the inverse square of the frequency when the radiation impedance is mainly resistive and the equivalent circuit is that shown in Fig. 6.6d.

6.5 THIELE–SMALL PARAMETERS [5]

A complete low-frequency model of a loudspeaker drive unit can be defined by just six parameters known as the Thiele–Small parameters, which are:

$$R_E,\ Q_{ES},\ Q_{MS},\ f_S,\ S_D,\ \text{and}\ V_{AS}.$$

So far, we have introduced all of these except for V_{AS}. The parameters Q_{ES}, Q_{MS}, f_S, and S_D are defined by Eqs. (6.11), (6.12), (6.8), and (6.22) respectively. The parameter V_{AS} is the *equivalent suspension volume*. In other words, it is the volume of air having the same acoustic compliance as the suspension and is defined as

$$V_{AS} = C_{AS}\rho_0 c^2 = C_{MS}S_D^2\rho_0 c^2 \tag{6.26}$$

The use of this parameter will make more sense when we consider the performance of the loudspeaker with an enclosure of volume V_B, which in its simplest approximation is an extra compliance in the loop of Fig. 6.4*b*. Straight away, we can say that mounting the drive unit in a box of volume $V_B = V_{AS}$ will result in a total compliance that is half that of the drive unit in free space or an infinite baffle. Hence, the suspension resonance frequency will be raised by a factor of $\sqrt{2}$. From these six parameters, we can furnish our equivalent circuit of Fig. 6.4*b* with all the required element values:

$$C_{MS} = \frac{V_{AS}}{S_D^2\rho_0 c^2} \tag{6.27}$$

Then from Eq. (6.8)

$$M_{MS} = \frac{1}{(2\pi f_S)^2 C_{MS}} \tag{6.28}$$

and from Eq. (6.12)

$$R_{MS} = \frac{1}{Q_{MS}}\sqrt{\frac{M_{MS}}{C_{MS}}} \tag{6.29}$$

Inserting Eq. (6.28) into Eq. (6.11) yields

$$Bl = \sqrt{\frac{R_E}{2\pi f_S Q_{ES} C_{MS}}} \tag{6.30}$$

where we have ignored R_g because this is not a drive unit parameter. Finally $M_{MD} = M_{MS} - 2M_{M1}$, where M_{M1} is given by Eq. (6.5). Another parameter that is commonly found in loudspeaker data sheets, although it is not a Thiele–Small parameter, is the maximum (linear) displacement or x_{max}. It is a difficult parameter to specify in any meaningful way because it depends on how much distortion can be tolerated and varies with frequency [6].

6.6 SOUND PRESSURE PRODUCED AT DISTANCE *r*

We show in Eq. (13.104) that the far-field on-axis pressure produced by a plane circular piston in an infinite baffle is given by

$$\begin{aligned}\tilde{p}(r) &= -jf\rho_0\tilde{U}_c\frac{e^{-jkr}}{r}\\ &= -\rho_0 S_D\tilde{a}_c\frac{e^{-jkr}}{2\pi r}\end{aligned} \tag{6.31}$$

where $\tilde{a}_c$ is given by Eqs. (6.8), (6.9), and (6.13) so that

$$\tilde{p}(r) = -\frac{\tilde{e}_g BlS_D\rho_0}{(R_g+R_E)M_{MS}}\cdot\frac{e^{-jkr}}{2\pi r}\alpha_c \tag{6.32}$$

The frequency response is then given by α_c in Eq. (6.14). In other words, the frequency response is proportional to the cone acceleration and remains flat above the suspension resonance.

The fact that the on-axis frequency response remains flat, even though the radiated power decreases when the wavelength is small in comparison to the circumference of the piston, may seem slightly surprising. However, what we have not taken into account here is the spatial distribution of the radiated sound pressure which becomes increasingly narrow at high frequencies. Although we are not dealing with an ideal flat piston and have not included the effect of the coil inductance, Eq. (6.32) is useful for defining the voltage sensitivity of a loudspeaker within its working frequency range between the suspension resonance and cone break-up (which we will discuss later in this chapter). It shows that for a given coil resistance R_E, the sensitivity is increased by maximizing the Bl factor and diaphragm area S_D while minimizing the total moving mass M_{MS}, which includes the radiation mass M_{MR}, although it is usually very small in comparison to M_{MD}. These requirements are usually in conflict with each other, so it is not possible to optimize all of them in a practical design. Since the most common nominal impedance of a loudspeaker is 8 Ω, the rms generator voltage $e_{g(\mathrm{rms})}$ is usually taken as $\sqrt{8}$ or 2.83 V_{rms} in order to deliver 1 W of power into an 8 Ω load. Hence, Eq. (6.32) can then be used to give the power sensitivity which is usually expressed in dB SPL [relative to 20 μPa, see Eq. (1.18)] for $W_E = 1$ W at $r = 1$ m, so that

$$\text{Sensitivity} = 20\log_{10}\left(\frac{\sqrt{Z_{\mathrm{nom}}W_E}BlS_D\rho_0}{2\pi r(R_g+R_E)M_{MS}\times 20\times 10^{-6}}\right)\ \text{dB SPL/W/m} \tag{6.33}$$

where Z_{nom} is the *nominal* electrical impedance of the drive unit. Theoretically, it is the average value over the loudspeaker's working frequency range, but in practice it is about 10–30% greater than R_E so that at some frequencies, especially those below resonance, more than 1 W will be supplied at the nominal voltage. Alternatively, by combining Eqs. (6.8), (6.11), (6.26), and (6.33) we may conveniently express the sensitivity in terms of the Thiele–Small parameters V_{AS} and Q_{ES}:

$$\text{Sensitivity} = 20\log_{10}\left(\frac{1}{rc\times 20\times 10^{-6}}\sqrt{\frac{Z_{\mathrm{nom}}W_E 2\pi f_S^3 V_{AS}\rho_0}{(R_g+R_E)Q_{ES}}}\right)\ \text{dB SPL/W/m} \tag{6.34}$$

Sometimes we wish to determine how far a diaphragm must travel to produce a target sound pressure level or SPL. From Eqs. (1.18) and (6.31) we obtain

$$\eta_{\text{peak}} = \frac{\sqrt{2}r \times 10^{\left(\frac{\text{SPL}}{20} - 5\right)}}{\pi f^2 \rho_0 S_D} \tag{6.35}$$

Low frequencies. From Eq. (13.101) we see that the magnitude of the pressure at a point in free space a distance r from *either* side of the loudspeaker in an infinite baffle is that of a point source multiplied by a directivity function:

$$\tilde{p}(r,\theta) = -jka^2\rho_0 c\tilde{u}_c \frac{e^{-jkr}}{2r} D(\theta), \tag{6.36}$$

where the directivity function $D(\theta)$ is given by

$$D(\theta) = \frac{2J_1(ka\sin\theta)}{ka\sin\theta}. \tag{6.37}$$

A piston whose diameter is less than one-third wavelength ($ka < 1.0$) is essentially nondirectional at low frequencies, that is $D(\theta) \approx 1$ for any value of θ. Hence, we can approximate it by a hemisphere whose volume velocity is $\tilde{U}_c = S_D\tilde{u}_c$. It is assumed in writing this equation that the distance r is great enough so that it is situated in the "far-field". Assuming a loss-free medium, the total radiated power distributed over a spherical surface in the far field is

$$W = 4\pi r^2 I = \frac{4\pi r^2}{\rho_0 c}\left|\frac{\tilde{p}(r)}{\sqrt{2}}\right|^2 \tag{6.38}$$

where I is the intensity at distance r in W/m^2. From this we see for a point source radiating to *both sides* of an infinite baffle (or free space) that

$$p_{\text{rms}}(r) = \sqrt{\frac{W\rho_0 c}{4\pi r^2}} \tag{6.39}$$

It is worth noting that it only takes 1 W of acoustic power to produce 6.7 Pa or 109 dB SPL at 1 m, which is as loud as a pneumatic drill! The fact that it takes much more than 1 W of input power to achieve this with a loudspeaker is due to the low efficiency of most loudspeakers.

Medium frequencies. At medium frequencies, where the radiation from the diaphragm becomes directional but yet where the diaphragm vibrates as one unit, i.e., as a rigid piston, the pressure produced at a distance r depends on the power radiated and the directivity factor Q.

The directivity factor Q was defined in Chapter 4 as the ratio of the intensity on a designated axis of a sound radiator to the intensity that would be produced at the same position by a point source radiating the same acoustic power.

For a directional source in an infinite baffle such as we are considering here,

$$p_{\text{rms}}(r) = \sqrt{\frac{W_1 Q\rho_0 c}{4\pi r^2}} \tag{6.40}$$

where

W_1 is acoustic power in W radiated from one side of the loudspeaker.
Q is directivity factor for *one* side of a piston in an infinite plane baffle. Values of Q are found from Fig. 4.30. Note that W_1 equals $W/2$ and, at low frequencies where there is no directionality, $Q = 2$, so that Eq. (6.40) reduces to Eq. (6.39) at low frequencies.

We see from Eq. (6.40) that, as frequency increases, Q increases while W_1 decreases. In other words, the reduction in radiated power is compensated for by the concentration of the radiated sound pressure over a decreasing beam width. The transition is so smooth that the frequency response remains flat. This can also be explained by the fact that the on-axis sound pressure is due to an infinite number of point sources over the surface of the piston, the radiation from which arrives in phase, where the frequency response of each point source is flat.

6.7 FREQUENCY-RESPONSE CURVES

A frequency-response curve of a loudspeaker is defined as the variation in sound pressure or acoustic power as a function of frequency, with some quantity such as voltage or electrical power held constant. In order to calculate the full frequency response, we refer to Fig. 6.4 but using Eqs. (13.116) to (13.118) for the exact acoustic radiation impedance. The total impedance in the loop with all quantities referred to the mechanical side is

$$\begin{aligned} Z_{MT} &= \frac{B^2 l^2}{R_g + R_E + j\omega L_E} + j\omega M_{MD} + R_{MS} + \frac{1}{j\omega C_{MS}} \\ &\quad + 2S_D \rho_0 c \left(1 - \frac{J_1(2ka)}{ka} + j \frac{\mathbf{H}_1(2ka)}{ka} \right) \end{aligned} \tag{6.41}$$

where $k = \omega/c$. The diaphragm velocity is then given by the driving force divided by the total impedance

$$u_{c(\mathrm{rms})} = \left| \frac{e_{g(\mathrm{rms})} Bl}{(R_g + R_E + j\omega L_E) Z_{MT}} \right| \tag{6.42}$$

We than calculate the on-axis pressure using

$$p_{\mathrm{rms}}(r) = \frac{\rho_0 f S_D u_{c(\mathrm{rms})}}{r} \tag{6.43}$$

and

$$\mathrm{SPL} = 20 \log_{10} \left(\frac{p_{\mathrm{rms}}(r)}{p_{ref}} \right) \tag{6.44}$$

where $p_{ref} = 20$ μPa rms. The on-axis pressure of a typical 100 mm loudspeaker in an infinite baffle is plotted in Fig. 6.7. For this application, the mass of the cone is made as light as possible and the

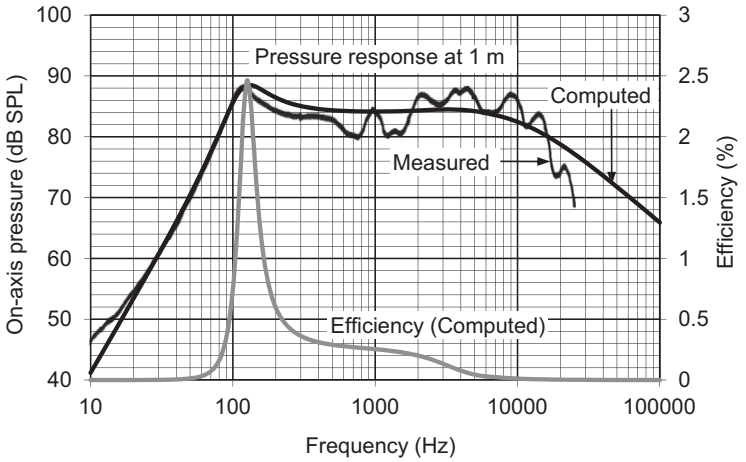

FIG. 6.7 On-axis pressure response and efficiency of an electrodynamic loudspeaker in an infinite baffle for which $e_{g(\text{rms})} = 2.83$ Vrms, $R_E = 7\ \Omega$, $L_E = 100\ \mu$H, $Q_{ES} = 2.2$, $Q_{MS} = 5$, $f_S = 125$ Hz, $S_D = 56$ cm^2, and $V_{AS} = 2$ L.

compliance of the suspension as high as possible consistent with mechanical stability. The high frequency response is aided by means of a concentric secondary or "whizzer" cone.

6.8 ELECTRICAL INPUT IMPEDANCE

If we ignore the radiation resistance, which is a negligibly small part of the input impedance, and add the radiation mass to the mechanical mass so that $M_{MS} = M_{MD} + 2M_{M1}$, we can write the electrical input impedance Z_E from inspection of Fig. 6.2:

$$Z_E = Z_{ES} + Z_{EM} = R_E + j\omega L_E + \left(j\omega \frac{M_{MS}}{B^2 l^2} + \frac{1}{B^2 l^2 G_{MS}} + \frac{1}{j\omega B^2 l^2 C_{MS}} \right)^{-1}$$

$$= R_E + j\omega L_E + \frac{B^2 l^2}{R_{MS}} \left(\frac{\frac{j}{Q_{MS}} \cdot \frac{f}{f_S}}{1 - \frac{f^2}{f_S^2} + \frac{j}{Q_{MS}} \cdot \frac{f}{f_S}} \right) \tag{6.45}$$

The electrical impedance curve of a typical 100 mm loudspeaker in an infinite baffle is plotted in Fig. 6.8. The peak at 125 Hz coincides with the suspension resonance frequency f_S. If we ignore the effect of the coil inductance L_E, the input impedance at f_S is approximately $Z_E = R_E + R_{ES}$ where $R_{ES} = B^2 l^2 / R_{MS}$ $(= R_E Q_{MS} / Q_{ES})$. Therefore a high peak indicates a large Bl factor or small mechanical damping resistance or both. At high frequencies, the impedance rises due to the increasing contribution of the coil inductance L_E. At very low frequencies, the impedance approaches the DC resistance R_E asymptotically, which in this case is 7 Ω.

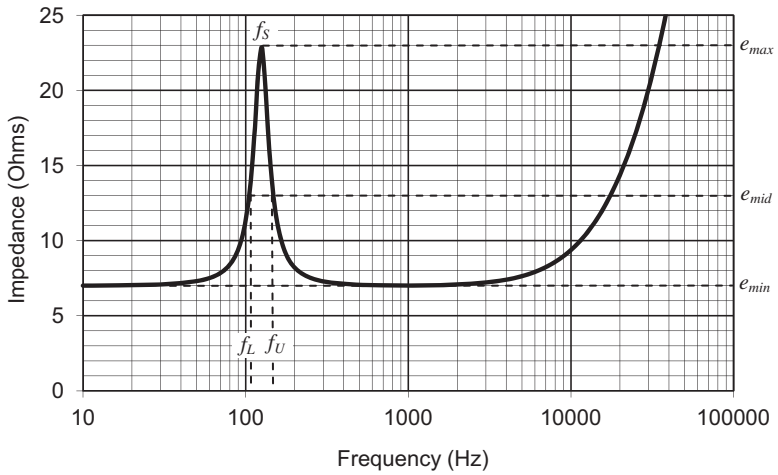

FIG. 6.8 Electrical impedance Z_E of an electrodynamic loudspeaker in an infinite baffle with the same parameters as those in Fig. 6.7.

6.9 EFFICIENCY

Medium frequencies. The efficiency of a loudspeaker is defined as 100 times the ratio of the acoustic power radiated to the power supplied by the electrical generator. In the medium frequency range between the suspension resonance and the point where the coil inductance starts to contribute to the electrical impedance, the power supplied by the generator is approximately

$$W_E \approx \frac{e^2_{g(\text{rms})}}{R_E} \tag{6.46}$$

where we are assuming that $R_g << R_E$. Using W from Eq. (6.23), the reference efficiency E_{ff} is then given by

$$E_{ff} = 100\frac{W}{W_E} \approx 100\frac{B^2 l^2 S_D^2 \rho_0}{\pi R_E M_{MS}^2 c}, \qquad 2f_0 < f < \frac{c}{4\pi a} \tag{6.47}$$

Not surprisingly, if we compare this with Eq. (6.32), we find that the same parameters which contribute to a high sound pressure level also make for an efficient loudspeaker, namely high field strength, low mass and a large radiating area. By combining Eqs. (6.8), (6.11), (6.26), and (6.47) we obtain a convenient expression for the reference efficiency in terms of Thiele–Small parameters:

$$E_{ff} = 100\frac{W}{W_E} \approx 100\frac{8\pi^2 V_{AS} f_S^3}{Q_{ES} c^3}, \qquad 2f_0 < f < \frac{c}{4\pi a} \tag{6.48}$$

At resonance. When $f = f_S$, the cone velocity is at a maximum value which is found by letting $X_M = 0$ in Eq. (6.1) so that

$$\tilde{u}_c = \frac{\tilde{e}_g Bl}{(R_g + R_E)R_M} \tag{6.49}$$

From Eqs. (6.19) and (6.21),

$$W = \frac{e_{g(\text{rms})}^2 B^2 l^2 \omega_S^2 S_D^2 \rho_0}{\pi c (R_g + R_E)^2 R_M^2} \tag{6.50}$$

The input power at resonance, assuming $R_{MS} >> 2\boldsymbol{R}_{MR}$, is given by

$$W_E = \frac{e_{g(\text{rms})}^2}{R_g + R_E + (B^2 l^2)/R_{MS}} \tag{6.51}$$

Then the efficiency at resonance, assuming $R_E >> R_g$, is given by

$$E_{ffS} = 100\frac{W}{W_E} = 100\frac{B^2 l^2 \omega_S^2 S_D^2 \rho_0}{\pi c (B^2 l^2 + R_E R_{MS}) R_{MS}} \tag{6.52}$$

Noting that $Q_{MS} = \omega_S M_{MS}/R_{MS}$ and $Q_{ES} = \omega_S M_{MS} R_E/(Bl)^2$, we obtain

$$E_{ffS} = 100\frac{W}{W_E} = 100\frac{Q_{ES} Q_{MS}^2 B^2 l^2 S_D^2 \rho_0}{(Q_{ES} + Q_{MS})\pi R_E M_{MS}^2 c} \tag{6.53}$$

Comparing this with Eq. (6.47) and using the relationship of Eq. (6.10) yields the following relationship between the efficiency at resonance E_{ffS} and the mid-band reference efficiency E_{ff}:

$$\frac{E_{ffS}}{E_{ff}} = Q_{TS} Q_{MS} \tag{6.54}$$

All frequencies. The power supplied by the generator at all frequencies is

$$W_E = e_{g(\text{rms})}^2 \Re\left(\frac{1}{Z_E}\right) \tag{6.55}$$

where the electrical impedance Z_E is given by Eq. (6.45). The radiated power is given by Eq. (6.19) where the cone velocity is given by Eq. (6.42) and $\boldsymbol{R}_{MR}$ by

$$\boldsymbol{R}_{MR} = S_D \rho_0 c \left(1 - \frac{J_1(2ka)}{ka}\right) \tag{6.56}$$

from Eq. (13.117). Hence

$$E_{ff} = 100\frac{W}{W_E} = 100\left|\frac{Bl}{(R_E + j\omega L_E)Z_{MT}}\right|^2 \frac{2S_D \rho_0 c}{\Re(1/Z_E)}\left(1 - \frac{J_1(2ka)}{ka}\right) \tag{6.57}$$

where Z_{MT} is given by Eq. (6.41). The efficiency of a typical 100 mm loudspeaker in an infinite baffle is plotted in Fig. 6.7. Not surprisingly, the loudspeaker is most efficient at the suspension resonance f_S where the input impedance is also at a maximum so that relatively little current is drawn. The

efficiency falls off at high frequencies due to diaphragm and coil inertia, where most of the input power is dissipated in heating the voice coil.

6.10 MEASUREMENT OF THIELE–SMALL PARAMETERS

Before embarking upon a loudspeaker enclosure design, we need to know the six Thiele–Small parameters that will be used to calculate the low-frequency response of our chosen drive unit in the enclosure. Most drive unit manufacturers now provide these on their datasheets, but if they are not available, we have to measure them. Even if they are available, production tolerances are such that we cannot always expect our computed frequency response to match the measured one unless the model used for computation is based on parameters obtained from the measured sample. In this section, it is shown how to obtain the Thiele–Small parameters purely by measuring the electrical input voltage at different frequencies using a multimeter and a calibrated variable-frequency oscillator.

During the tests, the electrodynamic loudspeaker is preferably mounted in a baffle such as the IEC 268-5 baffle [7], which is the standard baffle used by manufacturers. We see from Fig. 12.28 that if the outer diameter of the baffle is at least four times that of the loudspeaker, the radiation mass or reactive load is that of a piston in an infinite baffle. It should be borne in mind that if the loudspeaker is measured without any baffle, the radiation mass is halved which will result in a small error that can be corrected. It is not essential to perform the tests in an anechoic chamber: A large room that is not too noisy or reverberant will suffice. A variable-frequency source of sound with an output impedance R_g greater than 20 times the nominal impedance of the loudspeaker is connected to the loudspeaker terminals. An AC voltmeter is then connected across the terminals. The value of R_g should include both the inherent output impedance of the generator and any external resistor connected to in order to make up the desired impedance. The value of $e_{g(\text{rms})}$ is that measured by the meter before the loudspeaker is connected. Some AC meters are only designed to work at around 50–60 Hz, so it is worth checking to see if the reading varies with frequency with the loudspeaker disconnected. If it does, the open-circuit readings should be used to calibrate the measurements to the loudspeaker. The parameters are then determined as follows.

Measurement of suspension resonance frequency $\mathbf{f_S}$**.** In order to measure f_S, the frequency is varied until a maximum meter reading is obtained (see Fig. 6.9). From Fig. 6.2 and Fig. 6.8, we see that maximum electrical loudspeaker impedance corresponds to maximum mechanical admittance, which in turn occurs at the resonance frequency f_S or ω_S. The reading obtained at this frequency is e_{max}.

Measurement of $\mathbf{Q_{MS}}$ ***and*** $\mathbf{Q_{ES}}$**.** The minimum reading e_{min} in Fig. 6.8 is found by reducing the frequency until the voltage reading no longer changes. Increase the frequency again until the voltage

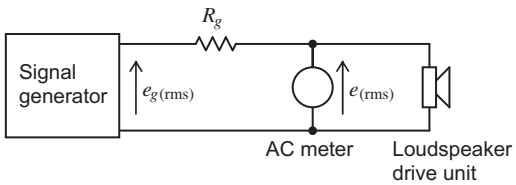

FIG. 6.9 Circuit for determining the Thiele–Small parameters of a loudspeaker.

reading gives a value of $e_{\text{mid}} = \sqrt{e_{\max} e_{\min}}$. The frequency at this point is f_L. Then increase the frequency beyond f_S (maximum voltage reading) until the voltage reading gives a value of $\sqrt{e_{\max} e_{\min}}$ for a second time. The frequency at this point is f_U. Note that $f_S = \sqrt{f_L f_U}$. The mechanical Q is then given by

$$Q_{MS} = \frac{f_S}{f_U - f_L} \left(\frac{e_g - e_{\min}}{e_g - e_{\max}} \right) \sqrt{\frac{e_{\max}}{e_{\min}}} \tag{6.58}$$

and the electrical Q by

$$Q_{ES} = \left(1 - \frac{e_{\max}}{e_g} \right) \frac{e_{\min} Q_{MS}}{e_{\max} - e_{\min}} \tag{6.59}$$

If the signal generator is a current source, then $e_g \to \infty$ and the bracketed terms become unity. These equations assume that the effect of the coil inductance L_E at around f_S is negligible.

***Measurement of* $\mathbf{R_E}$.** The electrical resistance of the voice coil is measured with a milliohm meter.

***Measurement of* $\mathbf{S_D}$.** The effective area of the diaphragm can be determined by coupling its front side to a closed box. The volume of air V_0 enclosed in the space bounded by the diaphragm and the sides of the box must be determined accurately. Then a slant manometer for measuring air pressure is connected to the airspace. The cone is then displaced a known distance ξ meters, the manometer is read, and the incremental pressure p is determined. Then,

$$p = \frac{P_0}{V_0} \xi S_D \tag{6.60}$$

or

$$S_D = \frac{P_0}{V_0} \frac{p}{\xi} \tag{6.61}$$

where P_0 is the ambient pressure. The pressures P_0 and p both must be measured in the same units, and V_0/ξ should be determined in m^2.

Usually, S_D can be determined accurately enough for most calculations from Fig. 6.1, that is, $S_D = \pi a^2$. In order to determine the effective radius a more accurately, we assume that the displacement of the surround(8) decreases linearly between its inner and outer edges which have radii a_1 and a_2 respectively. Then the effective radius is given by

$$a = \sqrt{\frac{a_1^2 + a_1 a_2 + a_2^2}{3}} \tag{6.62}$$

and the hence the effective area by

$$S_D = \frac{\pi}{3} (a_1^2 + a_1 a_2 + a_2^2) \tag{6.63}$$

***Measurement of* $\mathbf{V_{AS}}$.** The equivalent suspension volume V_{AS} [see Eq. (6.26)] can be obtained in two ways. Either we add mass to the diaphragm and observe the change in resonance frequency or we add stiffness in the form of a sealed enclosure. The first method is simplest and is suitable for most loudspeakers. However, in the case of micro speakers used in mobile devices, it is impractical to attach masses as the risk of destabilizing the diaphragm is too great.

The added mass is usually a rod of non-ferrous metal (e.g., enameled copper wire or solder) bent into a circle or spiral and attached to the diaphragm using tape or blu tack® so that it does not bounce.

If the original resonance frequency was f_S and the resonance frequency after addition of a mass M_x kg is f'_S, then

$$f_S = \frac{1}{2\pi\sqrt{M_{MS}C_{MS}}} \tag{6.64}$$

and

$$f'_S = \frac{1}{2\pi\sqrt{(M_{MS}+M_x)C_{MS}}} \tag{6.65}$$

where C_{MS} is mechanical compliance of the suspension in m/N. Simultaneous solution of (6.64) and (6.65) yields

$$M_{MS} = \frac{M_x}{(f_S/f'_S)^2 - 1} \tag{6.66}$$

Combining this with Eqs. (6.27) and (6.28) yields

$$V_{AS} = \left(1 - \frac{f'^2_S}{f^2_S}\right)\frac{S_D^2\rho_0 c^2}{(2\pi f'_S)^2 M_x} \tag{6.67}$$

Alternatively, if the drive unit is mounted in a sealed enclosure of known volume V_B, then the new resonance frequency is given by

$$f_C = \frac{1}{2\pi}\sqrt{\frac{C_{MS}+C_{MB}}{M_{MC}C_{MS}C_{MB}}} \tag{6.68}$$

where C_{MB} is the mechanical stiffness due to the air in the enclosure given by

$$C_{MB} = \frac{V_B}{S_D^2\rho_0 c^2} \tag{6.69}$$

Due to the air mass loading within the box, the total moving mass may be modified slightly, in which case we denote a new value M_{MC} and a new electrical Q_{EC}:

$$Q_{EC} = \frac{R_E}{B^2 l^2}\sqrt{\frac{M_{MC}(C_{MS}+C_{MB})}{C_{MS}C_{MB}}} \tag{6.70}$$

Simultaneous solution of Eqs. (6.11), (6.64), (6.68), and (6.70) yields

$$C_{MS} = \left(\frac{f_C Q_{EC}}{f_S Q_{ES}} - 1\right)C_{MB} \tag{6.71}$$

Hence from Eq. (6.27)

$$V_{AS} = \left(\frac{f_C Q_{EC}}{f_S Q_{ES}} - 1\right) V_B \tag{6.72}$$

In Chapter 7 of this book, on Loudspeaker Enclosures, design charts are presented from which it is possible to determine, without laborious computation, the sound pressure from a direct-radiator loudspeaker as a function of frequency including the directivity characteristics. Methods for determining the constants of box and bass-reflex enclosures are also presented. If the reader is interested only in learning how to choose a baffle for a loudspeaker, he or she may proceed directly to Chapter 7. The next part deals with the factors in design that determine the overall response and efficiency of the loudspeaker.

6.11 EXAMPLES OF LOUDSPEAKER CALCULATIONS

Example 6.1. Given the efficiency of Eq. (6.47) for a loudspeaker in an infinite baffle, determine the reference sound pressure equivalent to the efficiency assuming that the directivity factor Q (for radiation to one side) equals 2.

Solution. The sound pressure at distance r, assuming no directivity, is related to the acoustic power radiated to one side as follows [see Eqs. (6.40) and (6.46)]:

$$p_{\text{rms}}(r) = \sqrt{\rho_0 c I} = \sqrt{\frac{\rho_0 c W_1}{2\pi r^2}}$$

where

I is intensity at distance r
$W_1 = W/2$ is total acoustic power radiated from *one* side of the diaphragm.

The reference sound pressure is

$$p_{\text{rms}}(r) = \sqrt{\frac{\rho_0 c}{2\pi r^2}} \sqrt{\frac{E_{ff}}{200} W_E}$$

$$= \frac{e_{g(\text{rms})} \rho_0 B l S_D}{2\pi r R_E (M_{MD} + 2M_{M1})}$$

which is that given by Eq. (6.32) in the pass-band where $\alpha_c \approx 1$ and it is assumed that $R_g << R_E$.

Example 6.2. As an example of the efficiency to be expected from an electrodynamic loudspeaker of conventional design mounted in an infinite baffle and radiating directly from both sides of the baffle, let us calculate the reference efficiency E_{ff} from Eq. (6.48) for the case of a commercial loudspeaker with an advertised diameter of 10 cm. Also, let us calculate the ratio of the efficiency at the suspension resonance frequency to the reference efficiency. The values of the six Thiele–Small parameters are:

$R_E = 7\ \Omega$
$Q_{ES} = 2.2$
$Q_{MS} = 5$
$f_S = 125$ Hz

$S_D = 56\ \text{cm}^2$
$V_{AS} = 0.002\ \text{m}^3$ (2 Liters)

Also

$a = \sqrt{S_D/\pi} = 42.22\ \text{mm}$

$$Q_{TS} = \frac{Q_{ES}Q_{MS}}{Q_{ES} + Q_{MS}} = 1.528$$

ρ_0, density of air $= 1.18\ \text{kg/m}^3$
c, speed of sound $= 344.8$ m/s.

Solution. From Eq. (6.48), we obtain

$$E_{ff} = 100\frac{8 \times (3.14)^2 \times 0.002 \times (125)^3}{2.2 \times (344.8)^3} = 0.342\%$$

For radiation from one side of the loudspeaker only, divide this figure by 2. Hence only 0.171% of the available electrical power is radiated to one side of the diaphragm at mid to low frequencies. This illustrates the statement made at the beginning of the chapter that the efficiency of this type of loudspeaker is usually low.

For our example, the transition frequency at which the loudspeaker starts to become more directional and the efficiency decreases rapidly occurs when ka lies approximately between 1 and 2. For our example $ka = 1$ corresponds to a frequency of

$$f = \frac{c}{2\pi a} = \frac{344.8}{2\pi \times 0.04222} = 1.3\ \text{kHz}$$

Obviously, a smaller diaphragm of lighter weight would result in this transition extending to a higher frequency. However, a reduction in the mass M_{MD} occasioned by a smaller diaphragm will cause an increase in the first resonance frequency with a resulting loss in bass response. A further disadvantage of a smaller diaphragm is that, for a given sound pressure, a greater voice-coil velocity $\tilde{u}_c$ is needed. A longer air gap and a larger magnet structure must therefore he provided.

From Eq. (6.54), we obtain the efficiency at the suspension resonance:

$$E_{ffS} = 1.528 \times 5 \times 0.342 = 2.61\%$$

Hence, the ratio E_{ffS}/E_{ff} equals 7.64, and efficiency at f_S equals 1.3% for radiation from one side only.

PART XX: DESIGN FACTORS AFFECTING DIRECT-RADIATOR LOUDSPEAKER PERFORMANCE

A loudspeaker generally is designed to provide an efficient transfer of electric power into acoustic power and to effect this transfer uniformly over as wide a frequency range as possible. To accomplish this, the voice coil, diaphragm, and amplifier must be properly chosen. The choice of the elements and their effect on efficiency, directivity, and transient response are discussed here.

6.12 MAGNET SIZE

A cross-sectional sketch of a typical micro speaker is shown in Fig. 6.10. In this discussion, it is assumed that the coil fills the gap in the magnetic path without any air spaces and that it has the same permeability as free space. For the sake of argument, the wire cross-section might be rectangular so that any gap width or length could accommodate an integer number of turns or layers respectively. It is also assumed that the reluctances of the pole pieces are negligible in comparison with that of the gap, so these are ignored. The radii of the diaphragm, magnet, and coil are a, a_m, and a_c respectively.

Suppose the solid curve in Fig. 6.11 to represent the demagnetizing portion of the hysteresis loop for a magnetizing force H_{sat} obtained with the coil gaps in Fig. 6.10 closed, where B_R is the remanent flux density. To neutralize the residual magnetism, it is necessary to apply, by means of a suitable field winding, a demagnetizing magneto-motive force $\Im$ in ampere-turns. If H_C is the coercive force and l_m the length of the magnet, then $\Im = H_C l_m$. Therefore $\Im$ may be termed *the inherent magneto-motive force* for maintaining the remanent flux density B_R.

With the coil gaps in Fig. 6.10 closed, let us reduce the magnetic field strength from H_{sat} to zero and then increase it to H_1 in the reverse direction, so that the flux density is reduced to B_1. The net magneto-motive force available to produce this flux density in the magnet is $H_C l_m - H_1 l_m$ or in other words, the difference between the inherent MMF and applied MMF.

Next, let us gradually pull the pole-pieces apart and at the same time reduce the demagnetizing current in the field coil so as to keep the flux density constant at B_1. Suppose the procedure to be continued until the current has been reduced to zero and suppose l_g in Fig. 6.10 to be the corresponding gap length. Since this gap has been introduced without any change of flux density in the magnet, it follows that the magneto-motive force now available to send the flux ϕ across the gap is therefore $H_1 l_m$,

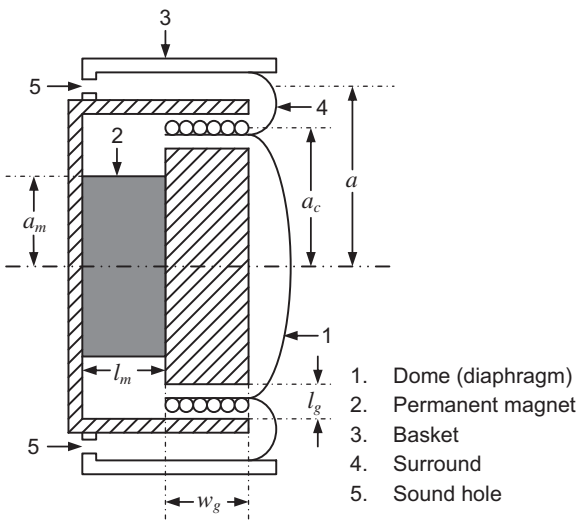

FIG. 6.10 Cross-sectional sketch of a micro speaker.

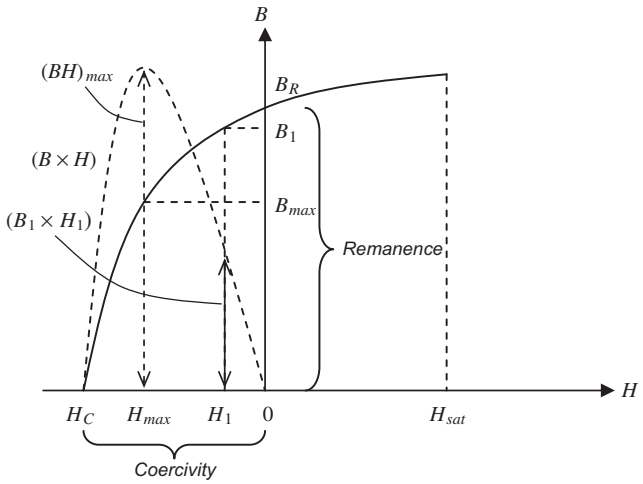

FIG. 6.11 A typical demagnetization curve.

namely that neutralized by the negative magneto-motive force of the field coil before the gap was introduced. The flux ϕ across the gap is given by

$$\phi = B_1 \pi a_m^2 = B_g \times 2\pi a_c w_g \tag{6.73}$$

where B_1 is the flux density in the magnet and B_g is the flux density in the gap. Also, the magneto-motive force required to send flux across the gap is given by

$$\Im_g = \frac{B_g l_g}{\mu_0}, \tag{6.74}$$

where $\mu_0 = 4\pi \times 10^{-7}$ H/m is the permeability of free space, but it was shown that the magneto-motive force required to send flux across the gap is given by $H_1 l_m$. Therefore

$$H_1 l_m = \frac{B_g l_g}{\mu_0}. \tag{6.75}$$

From Eqs. (6.73) and (6.75) it follows that the volume V_m of the magnet is given by

$$\begin{aligned} V_m &= \pi a_m^2 l_m \\ &= \frac{B_g \times 2\pi a_c w_g}{B_1} \cdot \frac{B_g l_g}{H_1 \mu_0} \\ &= \frac{2\pi a_c w_g l_g B_g^2}{\mu_0 B_1 H_1} \end{aligned} \tag{6.76}$$

From Eq. (6.76), it is evident that for a given flux density in the given dimensions of the gap, the volume of the magnet is a minimum when the product $B_1 H_1$ is a maximum. The variation of this

product with H in the *magnet core* is shown in Fig. 6.11 as a dashed curve from which it follows that the volume of the magnet is a minimum when it is operated at magneto-motive force H_{max}. The value of the product $(BH)_{max}$, also known as the *maximum energy product*, for a magnetic material is the best criterion of its suitability for use as a permanent magnet and the volume is then given by

$$V_m = \frac{2\pi a_c w_g l_g B_g^2}{\mu_0 (BH)_{\max}} \tag{6.77}$$

Notice that

$$V_g = 2\pi a_c w_g l_g \tag{6.78}$$

is the volume occupied by the gap. Also, let us assume that the field in the pole pieces is in saturation so that $B_g = B_{sat}$. This prevents the field from varying significantly with the driving current in the coil and thus improves linearity. Hence the magnet volume can be written as

$$V_m = \frac{B_{sat}^2}{\mu_0 (BH)_{\max}} V_g \tag{6.79}$$

If the demagnetization curve were perfectly linear, the values of H_{max} and B_{max} would be exactly half of the values of the coercivity and remanence respectively, which are more commonly found in manufacturer's data than H_{max} and B_{max}. However, due to nonlinearity a factor of 2/3 should give a reasonably good

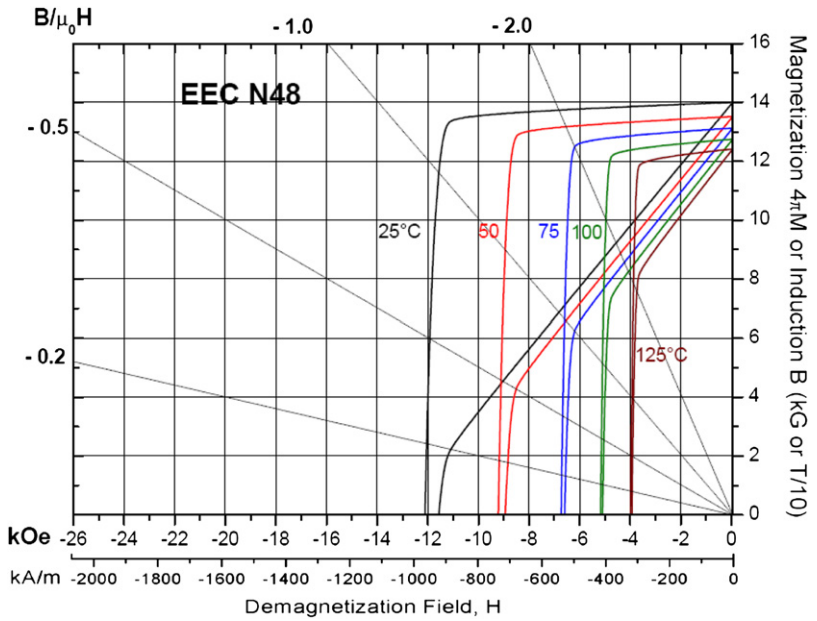

FIG. 6.12 Demagnetization curves for a commercial NdFeB magnet at 5 different temperatures ranging from 25°C to 125°C. Upper curves are intrinsic values and lower curves are actual values including applied field.

estimate for many materials, although neodymium iron boron (NdFeB) magnets [8] are remarkably close to ideal, as can be seen in Fig. 6.12. The upper curves are the *intrinsic B* versus *H* values which show the flux density excluding the flux due to the external applied field, and the lower curves are the *actual* "normal" *B* versus *H* values including the total net flux. It should be noted that the intrinsic coercivity is slightly greater than the actual coercivity. Commercial neodymium iron boron (NdFeB) magnets are denoted by a grade which specifies the maximum energy product in mega-gauss-oersteds and the minimum intrinsic coercivity in kilo-oersteds. For example, a Grade N4811 NdFeB magnet has a maximum energy product BH_{max} of 48 MGOe and a minimum intrinsic coercivity H_{ci} of 11 kOe. For our calculations, it is more convenient to use MKS units, in which case the conversions can be made using

$$1\ \text{G} = 10^{-4}\ \text{T} \tag{6.80}$$

$$1\ \text{Oe} = \frac{10^3}{4\pi}\ \text{A/m} \tag{6.81}$$

Hence, a Grade N4811 NdFeB magnet has a maximum energy product BH_{max} of 382 kTA/m and a minimum intrinsic coercivity H_{ci} of 875 kA/m.

6.13 VOICE-COIL DESIGN

Effect of coil size on efficiency. Let us now reconsider Eq. (6.47) to see how to maximize the efficiency in terms of the actual coil dimensions. The resistance R_E can be expressed in terms of the mass of the voice-coil winding M_{MC} by writing

$$R_E = \frac{\kappa\, l}{\pi\, a_w^2} \tag{6.82}$$

where

κ is resistivity of voice-coil conductor in units of $\Omega\cdot$m. The value of κ for different materials is given in Table 6.1.
a_w is radius of wire in m.
l is length of voice-coil winding in m.

We also note that the volume occupied by the coil wire is

$$V_w = \pi a_w^2 l \tag{6.83}$$

where for simplicity we are assuming that the space occupied by the coil former and insulation is negligible compared with the conductor. Inserting Eqs. (6.82) and (6.83) into Eq. (6.47) yields

$$E_{ff} \approx 100\frac{V_w B^2 S_D^2 \rho_0}{\pi\kappa M_{MS}^2 c}, \qquad 2f_0 < f < \frac{c}{4\pi a} \tag{6.84}$$

We now define the total moving mass by

$$M_{MS} = M'_{MS} + M_{MC} \tag{6.85}$$

Table 6.1 Resistivity and density of various metals

Metal element	Resistivity κ, 10^{-6} Ω·m	Density ρ_w, 10^3 kg/m^3	$\kappa\rho_w^2$, Ω·kg^2/m^5	Ranking
Aluminum	0.0283	2.70	0.206	6
Antimony	0.417	6.6	18.2	21
Bismuth	1.190	9.8	114.2876	27
Cadmium	0.075	8.7	5.68	14
Calcium	0.046	1.54	0.109	4
Carbon	8.0	2.25	40.5	25
Cesium	0.22	1.9	0.794	8
Chromium	0.026	6.92	1.25	9
Cobalt	0.097	8.71	7.36	19
Copper	0.0172	8.7	1.30	10
Gold	0.0244	19.3	9.09	20
Iridium	0.061	22.4	30.6	24
Iron	0.1	7.9	6.24	18
Lead	0.220	11.0	26.6	23
Lithium	0.094	0.534	0.0268	1
Magnesium	0.046	1.74	0.139	5
Manganese	0.050	7.42	2.75	12
Mercury	0.958	13.5	174	28
Molybdenum	0.057	10.2	5.93	15
Nickel	0.078	8.8	6.04	16
Platinum	0.10	21.4	45.8	26
Potassium	0.071	0.87	0.0537	3
Silver	0.0163	10.5	1.80	11
Sodium	0.046	0.97	0.0433	2
Tin	0.115	7.3	6.13	17
Titanium	0.032	4.5	0.648	7
Tungsten	0.055	19.0	19.9	22
Zinc	0.059	7.1	2.97	13

where M'_{MS} is the combined mass of the diaphragm and radiation load excluding the coil, and M_{MC} is the mass of the coil given by

$$M_{MC} \approx V_w \rho_w = \frac{\pi}{4} V_g \rho_w \tag{6.86}$$

where ρ_w is the density of the voice-coil wire in kg/m^3 (see Table 6.1). Inserting Eqs. (6.85) and (6.86) into Eq. (6.84) yields

$$E_{ff} \approx 100 \frac{V_w B^2 S_D^2 \rho_0}{\pi\kappa (V_w \rho_w + M'_{MS})^2 c}, \qquad 2f_0 < f < \frac{c}{4\pi a} \tag{6.87}$$

In order to find the optimum coil volume, we differentiate with respect to V_w and set the result to zero:

$$\frac{\partial}{\partial V_w}E_{ff} = 100\frac{(M'_{MS} - V_w\rho_w)B^2S_D^2\rho_0}{\pi\kappa(V_w\rho_w + M'_{MS})^3c} = 0 \tag{6.88}$$

so that the optimum coil volume is given by

$$V_w = M'_{MS}/\rho_w \tag{6.89}$$

Hence, the optimum mass for the coil is that of the diaphragm (less the coil) combined with the radiation mass. If the coil wire has a circular cross-section, then the gap volume is $V_g = 4V_w/\pi$, otherwise for a square cross-section $V_g = V_w$. Let us suppose for the sake of argument that we can make the diaphragm as light as we wish and that it remains perfectly rigid. Then setting $M'_{MS} = M_{MC}$ gives

$$E_{ff} \approx 100\frac{2B^2S_D^2\rho_0}{\pi^2\kappa\rho_w^2V_gc}, \qquad 2f_0 < f < \frac{c}{4\pi a} \quad M_{MS} \approx M_{MC} \tag{6.90}$$

From this equation we see that the efficiency is independent of the coil resistance, number of turns, or wire diameter. It is only dependent on the volume of the gap and the properties of the conductor, namely the resistivity κ and the density ρ_w. The product $\kappa\rho_w^2$ which appears in the denominator of Eq. (6.90) is given in Table 6.1 for various materials and ranked in ascending order. Unfortunately, the top-ranked four materials—lithium, sodium, potassium, and calcium—are not practicable for loudspeakers because they are highly reactive metals. Although copper is the material most commonly used in voice coils, there are many instances where aluminium has been successfully deployed to give increased efficiency and sensitivity. The problem in microspeakers is that aluminium lead out wires are somewhat brittle and liable to break after repeated flexing, although an alloy could be used. We have already deduced in Eq. (6.79) that the size of the magnet V_M is directly related to that of the magnetic gap V_G. Hence, reducing the gap volume not only makes the loudspeaker more efficient, but also reduces the required magnet size and therefore saves cost and weight.

Number of turns and wire diameter. The length l of the coil wire is

$$l = 2\pi a_c N \tag{6.91}$$

where N is the number of turns and the cross-sectional area S_w of the wire is

$$S_w = \pi a_w^2 = \frac{\pi w_g l_g}{4N} \tag{6.92}$$

Inserting Eqs. (6.91) and (6.92) into Eq. (6.82) for the coil resistance and solving for N yields

$$N = \sqrt{\frac{w_g l_g R_E}{8a_c\kappa}} \tag{6.93}$$

Then the wire radius is given by

$$a_w = \sqrt{\frac{w_g l_g}{4N}} = \left(\frac{V_g\kappa}{4\pi R_E}\right)^{1/4} \tag{6.94}$$

from Eqs. (6.78), (6.82), and (6.91). Therefore, we conclude that, whilst reducing the coil volume is beneficial for efficiency and reducing the magnet size, there is a limit to how much the volume can be reduced because eventually the wire becomes so thin that it is difficult to manufacture with any reasonable tolerance. Also, smaller coils are more difficult to cool, although with the increased efficiency they should not run so hot. Interestingly, the efficiency and wire radius are both independent of the coil geometry, and only dependent on its volume. This means there is a certain amount of flexibility regarding the diameter d or length l_g of the coil. Ideally, we would like to maximize l_g as this would also maximize the linear displacement x_{max}. In microspeakers, however, the gap length cannot be increased too much as the thickness of the component is an important factor in the design of the host product, especially if it is a mobile device. It is obvious from Eq. (6.94) that thinner wire is needed for high impedance loudspeakers in which R_E is large. However, reducing R_E usually results in greater losses in the amplifier and associated power source, so it is rarely less than about 3 Ω.

6.14 DIAPHRAGM BEHAVIOR

The simple theory using the method of equivalent circuits, which we have just derived, is not valid above some frequency between 300 and 1000 Hz. In the higher frequency range the cone no longer moves as a single unit, and the diaphragm mass M_{MD} and also the radiation impedance change. These changes may occur with great rapidity as a function of frequency. As a result, no exact mathematical treatment is available by which the performance of a loudspeaker can be predicted in the higher frequency range, unless the geometry is very simple, as in the case of a shallow spherical shell [9]. Cones are often approximated by concentric rings [10] or finite element models. Modern finite element models include the magnetic path and non-linear behavior [11].

A detailed study of one particular loudspeaker is reported here as an example of the behavior of the diaphragm [12]. The diaphragm is a felted paper cone, about 170 mm in effective diameter (see Fig. 6.13), having an included angle of 118°. The sound-pressure-level response curve for this loudspeaker measured on the principal axis is shown in Fig. 6.14.

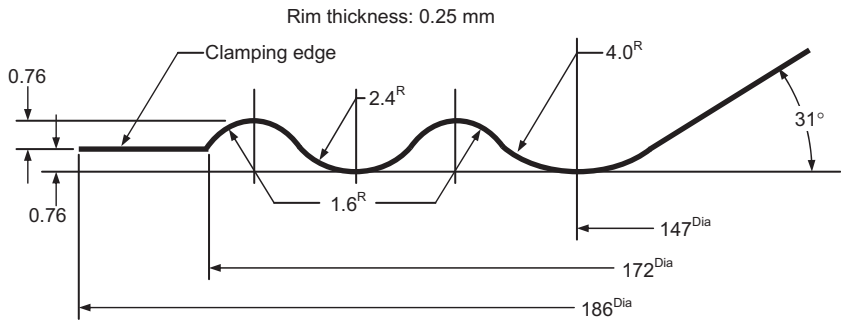

FIG. 6.13 Detail of the edge of a felted-paper loudspeaker cone from a 200 mm loudspeaker.

After Corrington, Amplitude and Phase Measurements on Loudspeaker Cones, *Proc. IRE*, **39:** 1021–1026 (1951).

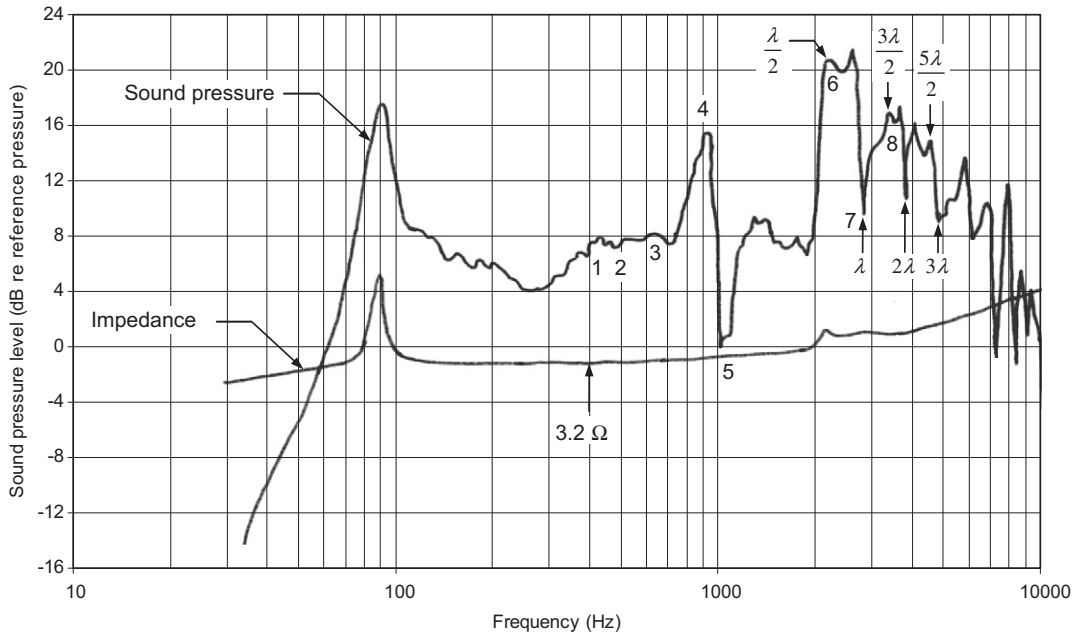

FIG. 6.14 On-axis response of a 200 mm diameter loudspeaker mounted in an infinite baffle.

After Corrington, Amplitude and Phase Measurements on Loudspeaker Cones, *Proc. IRE*, **39:** 1021–1026 (1951).

This particular loudspeaker has, in addition to its fundamental resonance, other peaks and dips in the response at points 1 to 8 as indicated on the curve. The major resonance at 90 Hz is the principal suspension resonance f_S and has the relative amplitude given by 20 log Q_{TS} from Eq. (6.14). Immediately above that is a fairly flat region. At point 1, which is located at 420 Hz, the cone breaks up into a resonance of the form shown by the first sketch in Fig. 6.15. Here, there are four nodal lines on the cone extending radially, and four regions of maximum movement. As indicated by the plus and minus signs, two regions move outward while two regions move inward. The net effect is a pumping of air back and forth across the nodal lines. The cone is also vibrating as a whole in and out of the page. The net change in the output is an increase of about 5 dB relative to that which it would be if the cone were perfectly rigid. A similar situation exists at point 2 at 500 Hz, except that the number of nodal lines is increased from 4 to 6. At point 3, 650 Hz, the vibration becomes more complex. Nodal lines are no longer well defined, and the speaker vibrates in such a way that the increase in pressure level is again about 5 dB.

For point 4 at 940 Hz, a new type of vibration has become quite apparent. The diaphragm moves in phase everywhere except at the rim. Looking at the rim construction shown in Fig. 6.13 and at the vibration pattern of Fig. 6.15(4), we can deduce what happens. The center part of the cone vibrates at a fairly small amplitude while the main part of the cone has a larger amplitude. At the 147 mm diameter the amplitude of vibration is very small. At this point the corrugation has a large radius (4 mm). As the cone moves to and fro, the paper tends to roll around this curve, and this excites the 2.4 mm corrugation that follows into violent oscillation at its resonance frequency. The rim resonance

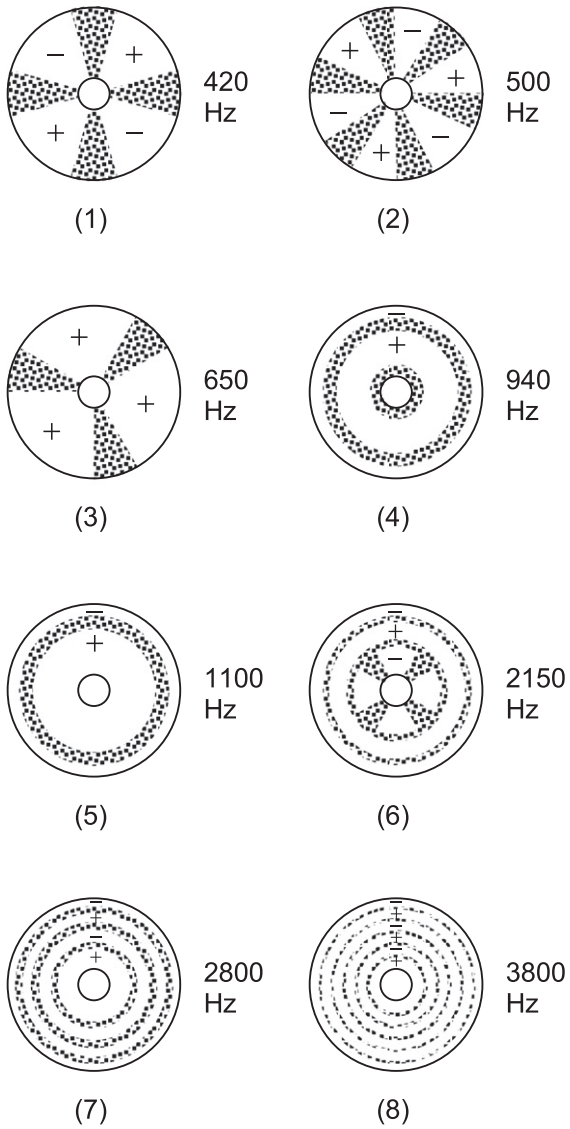

FIG. 6.15 Nodal pattern of the cone of the loudspeaker whose response curve is given in Fig. 6.14. The shaded and dashed lines indicate lines of small amplitude of vibration. The (+) and (−) signs indicate regions moving in opposite directions, i.e., opposite phases.

After Corrington, op. cit., with changes.

is 180° out of phase with respect to the main part of the cone. However, the main part of the cone has a high amplitude produced by the rocking motion around the 147 mm diameter, and because of its greater area, only part of its effect in producing a high sound level is canceled out by the rim motion. The net result is a peak in output (see point 4 of Fig. 6.14).

At point 5, 1100 Hz, a sharp decrease in response is observed. The decrease seems to be the result of a movement of the nodal line toward the apex of the cone, and a reduction of the amplitude of the (+) portion. Here, the effect is a pumping of air back and forth across the nodal line, with a cancellation in output. This vibration is very characteristic, and at the time such motion occurs, the response drops vigorously.

As frequency is increased, the loudspeaker breaks up into still different characteristic modes of vibration. As shown in Fig. 6.15, case 6, several nodal lines appear concentric to the rim of the loudspeaker. When these occur, a large increase in output is obtained, as shown at point 6 of Fig. 6.14. As frequency is increased, other such resonances occur, with more nodal lines becoming apparent. These nodal lines are the result of waves traveling from the voice coil out to the edge of the cone and being reflected back again. These outwardly and inwardly traveling waves combine to produce a standing-wave pattern that will radiate a maximum of power at some particular angle with the principal axis of the loudspeaker.

In order to reduce standing-wave patterns of the type shown in cases 6, 7, and 8 of Fig. 6.15, it is necessary that a termination of proper mechanical impedance be placed at the outer edge of the diaphragm. This termination must be one that absorbs waves traveling outward from the center of the cone so that no wave is reflected back. In practical design, a synthetic foam or rubber supporting edge is frequently employed. A rubber supporting edge is also effective in reducing the rim resonance. The resulting effect is to produce a more uniform response in the frequency region between 700 and 1500 Hz of Fig. 6.14.

The finite delay time it takes for higher frequency waves, which may be transverse or longitudinal, to travel through the cone from the edge of the voice coil to an absorbent surround has the effect of widening the directivity pattern, although the non-planar geometry of the cone also has this effect (see Sec. 12.10), but due to a phase advance towards the rim as opposed to a phase delay. In theory the two effects could be arranged to cancel each other so that the cone would act largely as a planar source, which would produce a maximally flat axial response, albeit with cup resonances and an increasingly narrow beam-width at high frequencies.

Often a highly damped cone material is chosen, such as paper, so that the waves propagating within it are absorbed at high frequencies. Consequently an ever decreasing portion of the cone radiates at high frequencies until the sound is coming mainly from the edge of the coil. If the mass of the coil were negligible compared to that of the cone, the moving mass would also progressively decrease with frequency and the radiated power would remain constant. Furthermore, the shrinking radiating area would maintain a wide directivity pattern as well as a flat on-axis response. Although this sounds like an ideal solution, greatest efficiency is actually obtained by making the coil and diaphragm masses equal (see Eq. (6.89)), so there is a limit to how much the total mass can decrease with frequency.

6.15 DIRECTIVITY CHARACTERISTICS

The response curve of Fig. 6.7 and the information of the previous three paragraphs reveal that, above the frequency where $ka = 2$ (usually between 800 and 2000 Hz), a direct-radiator loudspeaker can be

expected to radiate less and less power. The rate at which the radiated power would decrease, if the cone were a rigid piston, is between 6 and 12 dB for each doubling of frequency. This decrease in power output is not as apparent directly in front of the loudspeaker as at the sides because of directivity. That is to say, at high frequencies, the cone directs a larger proportion of the power along the axis than in other directions. Also, the decrease in power is overcome in part by the resonances that occur in the diaphragm, as we have seen from Fig. 6.14.

Directivity patterns for typical loudspeakers. Typical directivity patterns for a 5-inch-diameter direct-radiator loudspeaker, mounted in one of the two largest sides of a closed box having the dimensions 285 by 189 by 178 mm, were shown in Fig. 4.31. These data are approximately correct for loudspeakers of other diameters if the frequencies beneath the graphs are multiplied by the ratio of 5 inch to the diameter of the loudspeaker in inches.

Comparison with the directivity patterns for a flat rigid piston in a sphere, as shown in Fig. 12.23, reveals that the directivity patterns for a flat piston are different from those for an actual loudspeaker. This difference results from the cone angle, the speed of propagation of sound in the cone relative to that in the air, and the resonances in the cone. In this connection, it is interesting to see how the speed varies with frequency in an actual cone.

Speed of propagation of sound in cone. Let us define the average speed of propagation of sound in the cone as the distance between the apex and the rim, divided by the number of wavelengths in that distance, multiplied by the frequency in cycles per second. For the particular 200 mm loudspeaker of

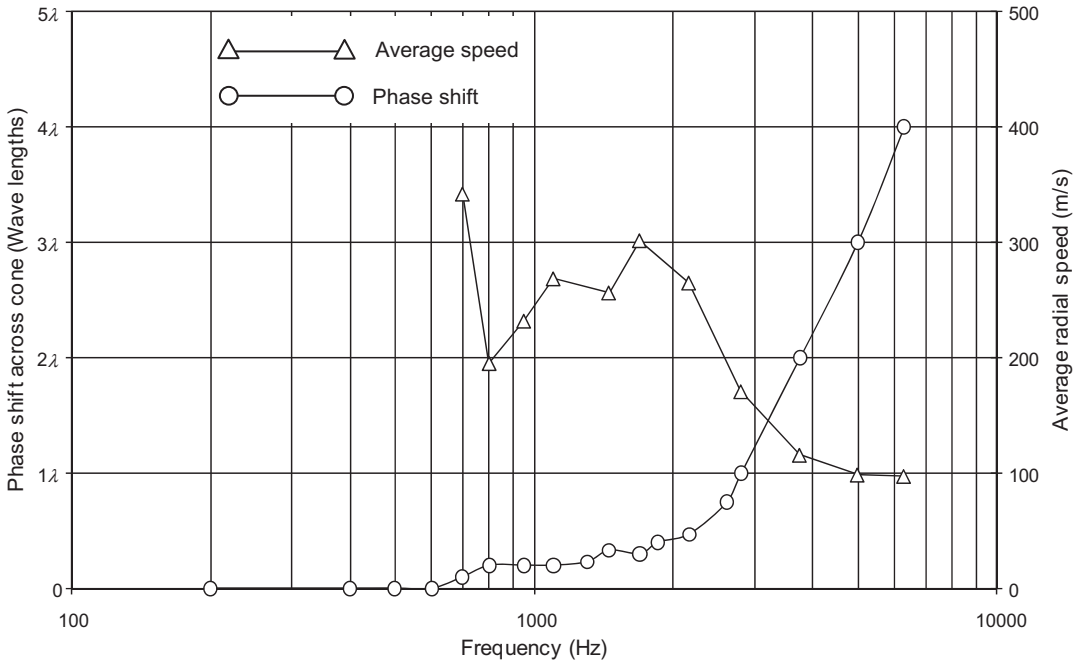

FIG. 6.16 Phase shift and average wave speed in the cone of a 200 mm loudspeaker.

After Corrington, Amplitude and Phase Measurements on Loudspeaker Cones, *Proc. IRE*, **39:** 1021–1020 (1951).

Fig. 6.13 to Fig. 6.15, the phase shift and the average speed of propagation of the sound wave from the apex to the rim of the cone are given in Fig. 6.16. At low frequencies the cone moves in phase so that the speed can be considered infinite. At high frequencies the speed asymptotically approaches that in a flat sheet of the same material, infinite in size.

Intensity level on designated axis. We have stated already that at high frequencies a loudspeaker diaphragm becomes directional. In order to calculate the enhancement of the sound pressure on the axis of the loudspeaker as compared with that indicated by Eqs. (4.65) and (4.66) for an omnidirectional source, it is convenient to use the concepts of directivity factor and of directivity index as defined in Part XII (pages 163 to 168). For example, we might wish to know the intensity (or the sound pressure level) on the axis of the loudspeaker, given the efficiency response and the directivity factor. This is done as follows.

The intensity as a function of frequency on the axis of symmetry of the loudspeaker divided by the electrical power available is equal to the product of (1) the efficiency response characteristic, (2) the directivity factor, and (3) $1/4\pi r^2$, where r is the distance at which the intensity is being measured. In decibels, we have

$$10 \log_{10} \frac{I_{ax}}{W_E} = 10 \log_{10} E_{ff} - 20 + \mathrm{DI} - 10 \log_{10} 4\pi r^2 \tag{6.95}$$

where

$I_{ax} = |p_{ax}|^2/\rho_0 c$ is intensity in watts per square meter on the designated axis at a particular frequency.
p_{ax} is sound pressure level in Pa measured on the designated axis at a particular frequency.
$E_{ff} = 100W/W_E$ is ratio of total acoustic power radiated by the front side of the loudspeaker to the power supplied by the electrical generator.

and where DI is given by Eq. (4.138) and Fig. 4.30. Note that, for the piston in an infinite baffle, the DI at low frequencies is 3 dB because the power is radiated into a hemisphere, and that the last term of Eq. (6.95) is the area of a sphere, in decibels.

Expressed in terms of the sound pressure level on the designated axis re 20 μPa, Eq. (6.95) becomes [see Eq. (6.40)]

$$\begin{aligned} \text{SPL } re \text{ 20 μPa}, = 20 \log_{10} \frac{p_{ax}}{0.00002} &= 10 \log_{10} W_E \\ &+ 10 \log_{10} E_{ff} + \mathrm{DI} - 10 \log_{10} 4\pi r^2 \\ &+ 10 \log_{10} \rho_0 c + 74 \text{ dB} \end{aligned} \tag{6.96}$$

6.16 TRANSFER FUNCTIONS AND THE LAPLACE TRANSFORM

If we substitute $s = j\omega$ in Eq. (6.14) we obtain

$$\alpha_c(s) = \frac{s^2}{s^2 + \dfrac{\omega_S}{Q_{TS}} s + \omega_S^2} \tag{6.97}$$

where s is the imaginary frequency variable. The roots of the denominator polynomial are known as *poles*. If $Q_{TS} \leq 0.5$, the roots of the denominator polynomial are real and given by

$$s = -\omega_S\left(\frac{1}{2Q_{TS}} \pm \sqrt{\frac{1}{4Q_{TS}^2} - 1}\right) \tag{6.98}$$

If $Q_{TS} > 0.5$, the roots of are complex and given by

$$s = -\omega_S\left(\frac{1}{2Q_{TS}} \pm j\sqrt{1 - \frac{1}{4Q_{TS}^2}}\right) \tag{6.99}$$

or expressed as magnitude and phase as

$$s = -\omega_S \angle \pm \arccos\left(1/(2Q_{TS})\right).$$

The dotted curves in Fig. 6.17 are plotted from Eq. (6.97), but solid lines are linear approximations plotted from the poles or roots of the denominator polynomial. The locus of these poles is shown in Fig. 6.18. The arrows on the negative real axis show the direction in which the poles move as Q_{TS} is increased. When $Q_{TS} = 0.5$, the poles are real and coincident at $-\omega_S$. When $Q_{TS} > 0.5$ they become a complex conjugate pair and follow the arrows on the semi-circular path. If there were no damping such that $Q_{TS} = \infty$, the poles would lie on the imaginary axis.

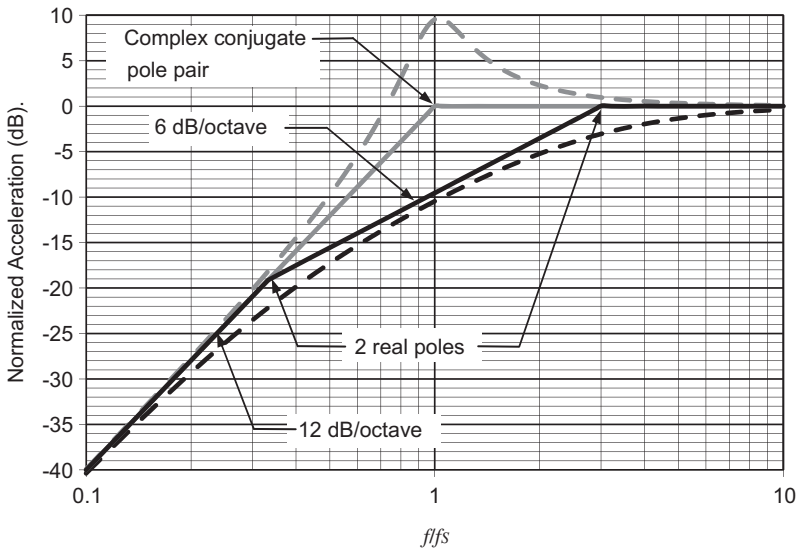

FIG. 6.17 Linear approximations of the acceleration frequency response function.

The black curves are for $Q_{TS} = 0.3$ and the gray for $Q_{TS} = 3$. The solid lines are linear approximations and the dotted curves are calculated from the exact expressions.

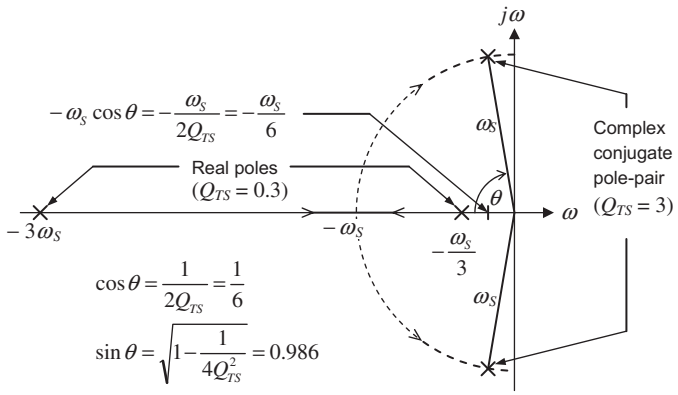

FIG. 6.18 Root loci of the poles in Fig. 6.17.

A more general transfer function is represented by

$$F(s) = \frac{Q_N s^N + Q_{N-1}s^{N-1} + \cdots + Q_2 s^2 + Q_1 s + Q_0}{P_M s^M + P_{M-1}s^{M-1} + \cdots + P_2 s^2 + P_1 s + P_0} = \frac{\sum_{n=0}^{N} Q_n s^n}{\sum_{m=0}^{M} P_m s^m} \tag{6.100}$$

which includes N *zeros* in the numerator as well as M poles in the denominator. Although we are unlikely to encounter zeros when dealing with larger loudspeakers, they do occur in cellphone designs which are generally more complicated, having small sound holes with viscous losses. Certainly, when we consider loudspeakers in bass-reflex enclosures or with auxiliary filters we will encounter higher order denominator polynomials. After solving the denominator and numerator polynomials for the poles p_m and zeros q_n respectively, we can rewrite the transfer function as

$$F(s) = \frac{(s+q_1)(s+q_2)\cdots(s+q_{N-1})(s+q_N)}{(s+p_1)(s+p_2)\cdots(s+p_{M-1})(s+p_M)} = \frac{\prod_{n=1}^{N}(s+q_n)}{\prod_{m=1}^{M}(s+p_m)} \tag{6.101}$$

This is a convenient form which enables us to tailor the frequency response by manipulating the roots of the denominator polynomial and to calculate the transient response by means of the inverse Laplace transform.

6.17 TRANSIENT RESPONSE

The design of a loudspeaker enclosure and the choice of amplifier impedance eventually must be based on subjective judgments as to what constitutes "quality" or perhaps simply on listening "satisfaction." It is believed by many observers that a flat sound-pressure-level response over at least the frequency range between 70 and 7000 Hz is found desirable by most listeners. Some observers believe that the response should be flat below 1000 Hz but that between 1000 and 4000 Hz it should be about 5 dB higher than its below-1000-Hz value. Above 4000 Hz, the response should return to its low-frequency value. It is also believed by some observers that those loudspeakers which sound best generally

reproduce tone bursts [13] well, although this requirement is better substantiated in the literature for the high frequencies than for the low.

An important factor determining the transient response of the circuits of Fig. 6.4 is the amount of damping of the motion of the loudspeaker diaphragm that is present. For a given loudspeaker, the damping may be changed (1) by choice of the amplifier impedance R_g, or (2) by adjustment of the resistive component of the impedance of the enclosure for the loudspeaker, or (3) by choosing a drive unit with a smaller Q_{TS} value, or (4) by any combination of (1) to (3). The amplifier impedance may be adjusted using negative current feedback to increase Q_{TS} or positive current feedback to reduce it. The latter provides a negative output impedance which is subtracted from R_E.

Before we can apply the transform to Eq. (6.101), we must split the expression into a sum of partial fractions, each containing a single factor in its denominator:

$$F(s) = \frac{A_1}{s+p_1} + \frac{A_2}{s+p_2} + \cdots + \frac{A_{M-1}}{s+p_{M-1}} + \frac{A_M}{s+p_M} = \sum_{m=1}^{M} \frac{A_m}{s+p_m} \tag{6.102}$$

This is achieved using a technique known as the residues theorem. The residues A_m are found from the formula

$$A_m = (s+p_m)F(s)\Big|_{s\to -p_m} \tag{6.103}$$

For the expression of Eq. (6.97) this gives

$$\begin{aligned} \alpha_c(s) &= \frac{s^2}{(s+p_1)(s+p_2)} \\ &= (1) + \frac{p_1^2}{(p_2-p_1)(s+p_1)} + \frac{p_2^2}{(p_1-p_2)(s+p_2)} \end{aligned} \tag{6.104}$$

The extra unity term in parentheses comes from the fact that the numerator polynomial is of the same order as the denominator. However, we shall drop it from subsequent handling. If $M < N$, then this term vanishes anyway. The poles p_1 and p_2 are given by

$$p_1 = \omega_S\left(\frac{1}{2Q_{TS}} - j\sqrt{1-\frac{1}{4Q_{TS}^2}}\right) \tag{6.105}$$

$$p_2 = \omega_S\left(\frac{1}{2Q_{TS}} + j\sqrt{1-\frac{1}{4Q_{TS}^2}}\right) \tag{6.106}$$

In order to obtain the response in the time domain, we apply the inverse Laplace transform:

$$f(t) = L^{-1}(F(s)) = \frac{1}{2\pi j}\int_{\gamma\text{-j}\infty}^{\gamma+j\infty} F(s)e^{st}ds \tag{6.107}$$

Table 6.2 Laplace transforms of various functions of time

f(t)	$\delta(t)$	$H(t)$	$\sin \omega t$	$\cos \omega t$	$e^{-\omega t}$	$1 - e^{-\omega t}$	$\frac{\alpha e^{-\alpha t} - \beta e^{-\beta t}}{\alpha - \beta}$	$1 - \frac{\alpha e^{-\beta t} - \beta e^{-\alpha t}}{\alpha - \beta}$
F(s)	1	$\frac{1}{s}$	$\frac{\omega}{s^2 + \omega^2}$	$\frac{s}{s^2 + \omega^2}$	$\frac{1}{s + \omega}$	$\frac{\omega}{s(s + \omega)}$	$\frac{s}{(s + \alpha)(s + \beta)}$	$\frac{\alpha\beta}{s(s + \alpha)(s + \beta)}$

where γ is an arbitrary positive constant chosen so that the contour of integration lies to the right of all singularities in $F(s)$. The Laplace transform is a variant of the Fourier transform that converts a function of time to one of imaginary frequency as opposed to real frequency.

$$F(s) = L(f(t)) = \frac{1}{2\pi j} \int_0^\infty f(t) e^{-st} ds \tag{6.108}$$

Table 6.2 shows the Laplace transforms of some input waveforms that we may wish to use to investigate the time response of a loudspeaker system with its associated enclosure and electrical filters.

We see that the Laplace transform of an infinite impulse at $t = 0$, which is represented by the Dirac delta function $\delta(t)$, is simply unity. Therefore applying the inverse Laplace transform directly to the frequency response function in s will give us the infinite impulse response of the system. Applying the inverse Laplace transform to Eq. (6.104) is fairly straightforward since according to Table 6.2 the $1/(s + p_m)$ terms become exponents:

$$\alpha_c(t) = \frac{p_1^2}{(p_2 - p_1)} e^{-p_1 t} + \frac{p_2^2}{(p_1 - p_2)} e^{-p_2 t} \tag{6.109}$$

If we wish to evaluate the time response to an input wave form other than an infinite impulse, we may multiply Eq. (6.104) by the Laplace transform of the waveform before applying the inverse Laplace transform. For example, if we wished to evaluate the response to a Heaviside step function $H(t)$, which represents a step from 0 to 1 at $t = 0$, we could multiply Eq. (6.104) by $1/s$ before applying the inverse Laplace transform. Alternatively, we could convolve the impulse response of Eq. (6.109) with the Heaviside step function in the time domain using the convolution integral:

$$\begin{aligned} \alpha_c(t) * H(t) &= \int_{-\infty}^{\infty} \alpha_c(x) H(t - x) dx \\ &= \frac{p_1 e^{-p_1 t} - p_2 e^{-p_2 t}}{p_1 - p_2} \\ &= \begin{cases} \dfrac{\sin(\theta - \omega_S t \sin\theta)}{\sin\theta} e^{-\omega_S t \cos\theta}, & Q_{TS} > 0.5 \\ \dfrac{\sinh(\theta - \omega_S t \sinh\theta)}{\sinh\theta} e^{-\omega_S t \cosh\theta}, & Q_{TS} \le 0.5 \end{cases} \end{aligned} \tag{6.110}$$

where

$$\cos\theta = \frac{1}{2Q_{TS}}, \qquad \sin\theta = \sqrt{1-\frac{1}{4Q_{TS}^2}}, \qquad Q_{TS} > 0.5 \tag{6.111}$$

$$\cosh\theta = \frac{1}{2Q_{TS}}, \qquad \sinh\theta = \sqrt{\frac{1}{4Q_{TS}^2}-1}, \qquad Q_{TS} \le 0.5 \tag{6.112}$$

which gives the same result as multiplying Eq. (6.104) by $1/s$ before applying the inverse Laplace transform. Hence the impulse response is a powerful expression which can be used to predict the response to any input waveform.

We see from Eq. (6.110) that when $Q_{TS} > 0.5$, the time response to a step function has an oscillatory component represented by the sine and cosine functions of $\omega_S t$ and a decaying component represented by the exponent term which contains the *decay constant* $\omega_S/(2\,Q_{TS})$. The response to a step function is plotted in Fig. 6.19 with $f_S = 50$ Hz. The black curve for $Q_{TS} = 3$ gives an undershoot value of 62% and ringing for several cycles, each about 20 ms in duration. They grey curve for $Q_{TS} = 0.3$ shows just 6.4% undershoot and no ringing.

An input waveform of particular interest is that of a finite tone burst* of frequency ω_0 and duration t_0 involves a somewhat more complicated expression:

$$F(t) = (1 - H(t - t_0))\sin\omega_0 t \tag{6.113}$$

which yields the pressure waveform

$$\begin{aligned} a_c(t) * F(t) = {} & \left(\omega^4 + \omega_S^4 + 2\omega^2\omega_S^2\cos 2\theta\right)^{-1} \\ & \times\left\{\csc\theta\left(\omega\omega_S^3\sin(\omega_S t\sin\theta) + \omega^3\omega_S\sin(\omega_S t\sin\theta - 2\theta)\right)e^{-\omega_S t\cos\theta} + H(t-t_0)\right. \\ & \times\left\{\csc\theta\sin\omega t_0\left(\omega_S^4\sin(\omega_S(t-t_0)\sin\theta - \theta) + \omega^2\omega_S^2\sin(\omega_S(t-t_0)\sin\theta - 3\theta)\right)\right. \\ & -\csc\theta\cos\omega t_0\left(\omega\omega_S^3\sin(\omega_S(t-t_0)\sin\theta) + \omega^3\omega_S\sin(\omega_S(t-t_0)\sin\theta - 2\theta)\right)\Big\} \\ & \times e^{-\omega_S(t-t_0)\cos(\theta)} + (1 - H(t-t_0))\left(2\omega^3\omega_S\cos\theta\cos\omega t + \omega^2(\omega^2 - \omega_S^2)\sin\omega t\right)\Big\} \end{aligned} \tag{6.114}$$

We see from Fig. 6.20 that the beginning of the tone burst excites the suspension resonance frequency which is superimposed upon the tone burst even though the tone-burst frequency is three times higher than that of the suspension resonance. As a result, the tone takes a while to settle before it is switched off, at which point the suspension resonance is triggered again before finally decaying. Hence, loudspeakers with a high Q_{TS} tend to produce bass with a "one-note" quality. Not only is the suspension resonance frequency boosted in the frequency response, but it also adds overhang to transients at other frequencies.

It is known that the reverberation time in the average living room is about 0.5 s, which corresponds to a decay constant of 13.8 s^{-1}. Psychological studies also indicate that if a transient sound in a room has decreased to less than 0.1 of its initial value within 0.1 s, most listeners are not disturbed by the

*A tone burst is a wave-train pulse that contains a number of waves of a frequency.

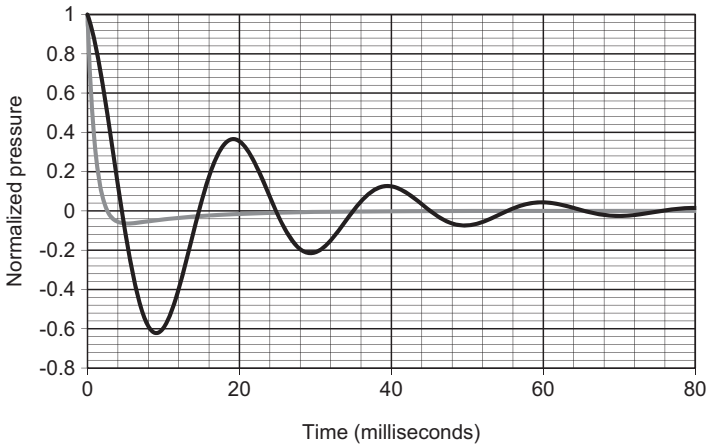

FIG. 6.19 Time response to a unity step function where $f_S = 50$ Hz.

The black curve is for $Q_{TS} = 3$. and the gray for $Q_{TS} = 0.3$.

"overhang" of the sound. This corresponds to a decay constant of 23 s^{-1}, which is a more rapid decay than occurs in the average living room. Although criteria for acceptable transient distortion have not been established for loudspeakers, it seems reasonable to assume that if the decay constant for a loudspeaker is greater than four times this quantity, i.e., greater than 92 s^{-1}, no serious objection will be met from most listeners to the transient occurring with a tone burst. Accordingly, the criterion that is suggested here as representing satisfactory transient performance is

$$\frac{\omega_S}{2Q_{TS}} > 92 \text{ s}^{-1} \tag{6.115}$$

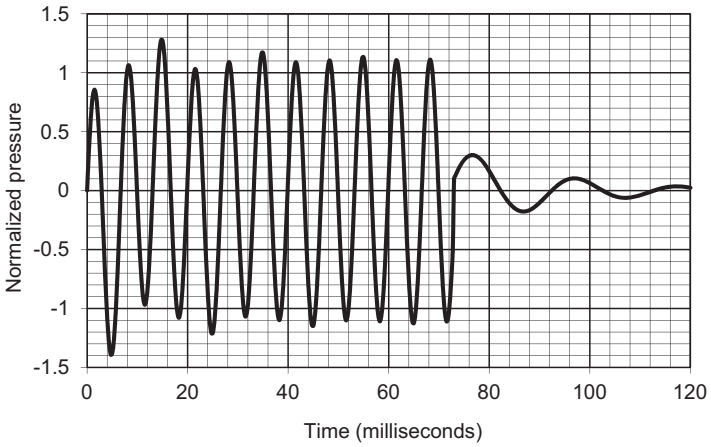

FIG. 6.20 Transient response to a tone burst of frequency $f_0 = 150$ Hz and duration $t_0 = 73$ ms, where the suspension resonance frequency $f_S = 50$ Hz and $Q_{TS} = 3$.

Equation (6.110) reveals that, the greater $\omega_S/(2\ Q_{TS})$, the shorter the transient. Equation (6.115) should be construed as setting a lower limit on the amount of damping that must be introduced into the system. It is not known how much damping ought to be introduced beyond this minimum amount.

In the next chapter we shall discuss the relation between the criterion of Eq. (6.115) and the response curve with baffle.

Each of the diaphragm resonances (e.g., points 1 to 8 in Fig. 6.14) has associated with it a transient decay time determined from an equation like Eq. (6.110). In order to fulfill the criterion of Eq. (6.115), it is usually necessary to damp the loudspeaker cone and to terminate the edges so that a response curve smoother than that shown in Fig. 6.14 is obtained. With the very best direct-radiator loudspeakers, much smoother response curves are obtained. The engineering steps and the production control necessary to achieve low transient distortion and a smooth response curve may result in a high cost for the completed loudspeaker.

6.18 NONLINEARITY [14]

There are a number of nonlinear mechanisms in electrodynamic loudspeakers which give rise to harmonic distortion. They tend to be dominant at different frequencies. In some cases the non-linearity is a function of input current and in others of displacement, or even both. An overview is given in Table 6.3.

Suspension compliance. The purpose of the suspension [see (9) in Fig. 6.1] is to provide a linear restoring force that moves the coil back to its rest position and to ensure that it is correctly centered.

Table 6.3 Overview of nonlinearities in electrodynamic loudspeakers

Nonlinearity	As a function of	Frequency range	Mechanism
Compliance C_{MS}	Displacement x	Below f_S	Nonlinear restoring force
Force factor Bl	Displacement x, current i	Low frequencies (where x is greatest)	Nonlinear force, $f = Bli$
	Displacement x, velocity u		Nonlinear damping, $e = Blu$
Coil inductance L_E	Displacement x	High freq. modulated by low freq.	Inductance varies with position of coil relative to pole-piece
	Displacement x, current i	Ditto	Extra reluctance force, $f \propto i^2$
	Current i	High frequencies	Nonlinear permeability of steel
Coil resistance R_E	Current i	All frequencies	Resistance increases with temp.
Young's modulus E of cone material	Strain ε	At normal vibration mode frequencies of cone	Stress σ is nonlinear function of strain, $\sigma = E\varepsilon$. For large amplitude vibrations, further nonlinearity caused by change in geometry.
Doppler effect	Displacement x	High freq. modulated by low freq.	Variable time shift $t = x/c$ in propagated sound causes freq. modulation distortion

However, from Fig. 6.21a we see that for large excursions, the suspension becomes stiffer as it stretches and so the compliance becomes nonlinear, typically in an asymmetrical manner, as shown in Fig. 6.21b. It is also common for hysteresis losses to prevent the coil from returning to the same position as before. In order to combat this, a "regressive" spider design [15] has been proposed in which the corrugations diminish in height with increasing radius.

Force factor. If the coil length h_c is equal to the gap length h_g (see Fig. 6.22a), the force factor decreases as soon as the coil starts to move in the x direction because the part of the coil which is then outside the gap experiences a much smaller force. This typically produces the dashed curve shown in Fig. 6.22b. In order to improve linearity and to extend the maximum excursion, the length of the coil is often extended beyond the length of the gap and this is known as *overhang*. This typically produces the solid curve shown in Fig. 6.22b. Alternatively, it can be shorter, which is known as *underhang*. One disadvantage of overhang is that the ratio of force factor Bl to moving mass M_{MS} is decreased, which tends to reduce efficiency somewhat (see Eq. (6.47)). Although

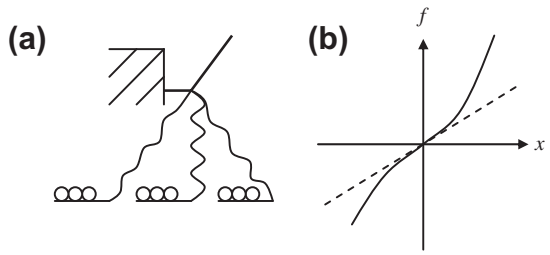

FIG. 6.21 (a) Sketch of suspension at center and extreme end positions and (b) non-linear force vs. displacement curve (solid curve) with ideal linear curve (dashed line).

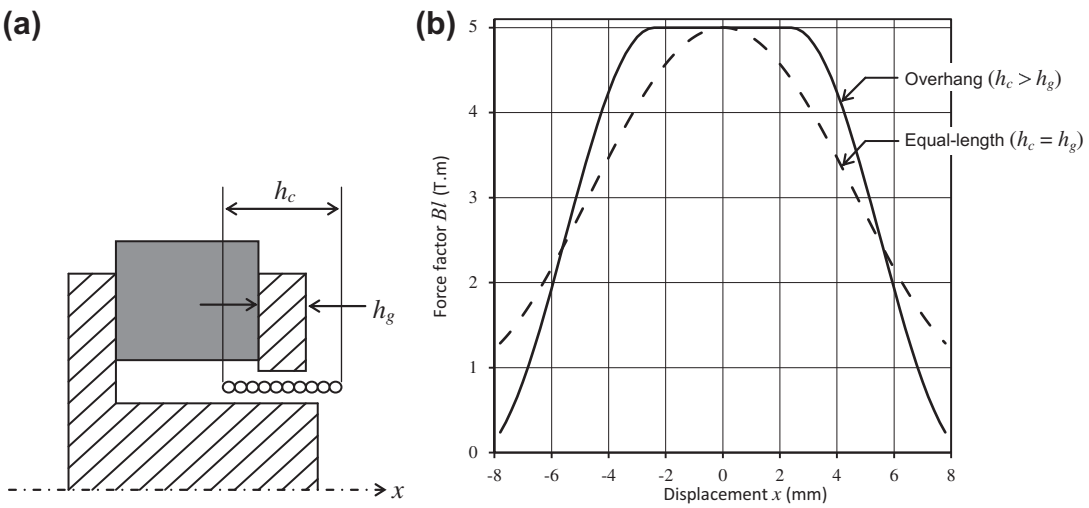

FIG. 6.22 (a) Sketch of a coil of lengh h_c in a magnetic gap of length h_g and (b) force factor vs. displacement curves with $h_c = h_g$ (dashed line) and $h_c > h_g$ (solid line).

force-factor nonlinearity is most noticeable at low frequencies, where the coil excursion is greatest, if the Q_{TS} value of the drive unit is fairly high then the distortion has a minimum at the suspension resonance frequency. In other words, the peak at the resonance frequency has a filtering effect on the distortion harmonics. By the same token, distortion harmonics of frequencies in the roll-off region (below resonance) are augmented.

Coil inductance. Like the force factor Bl, the coil inductance L_E also varies according to the position of the coil in the gap, albeit in a somewhat less symmetrical manner. In fact the inductance is greatest when the coil is in its innermost position and completely surrounded by iron, as we see from Fig. 6.23. Conversely it is smallest when the coil is in its outermost position and partly surrounded by air, which has a much smaller relative permeability than iron. Although the inductance alone would only affect the high frequencies, the fact that the excursion is greatest at low frequencies means that the effect of the nonlinearity is for the low frequencies to modulate the high frequencies.

Not only does the inductance vary with coil position x, but it also varies with current i. The flux density B varies in a nonlinear fashion with the magnetizing force H (see Fig. 6.11) and hence in turn with the current i. In order to minimize this effect, the pole piece and pole plate are normally saturated as much as possible so that there is relatively little variation of B with H. Also, the inclusion of a shorting ring around the pole piece, as shown in Fig. 6.23, reduces the variation of L_E with both x and i. It is usually made of aluminum and behaves like a short-circuited secondary winding of a transformer in which the voice coil forms the primary.

A third nonlinear mechanism due to the coil inductance is the reluctance force. This was actually the driving force used in the receivers of early telephone handsets. In the receiver, an electromagnet would actuate a steel plate in close proximity to it. Then the first loudspeakers were simply receivers with horns attached. Although the transduction was inherently nonlinear, the vibrations of the plate were small enough for the distortion not to be too serious. However, in a modern dynamic speaker, such a driving force is an undesirable byproduct of the principal transduction mechanism.

Coil resistance. As the power dissipated by the coil is increased, its temperature also increases, which leads to an increase in resistance. At very low frequencies, the temperature increases during every half cycle of the input signal, thus leading to odd harmonic distortion. At higher frequencies, the thermal inertia of the coil smoothes out the temperature variations so that instead we have a phenomenon known as *power compression* whereby the rise in coil resistance temporarily reduces the sensitivity of

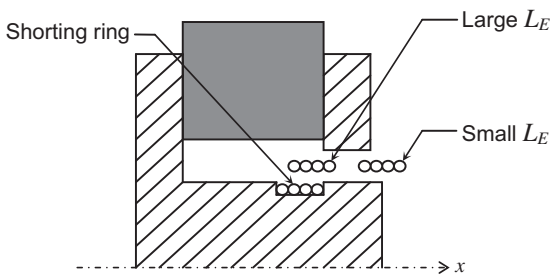

FIG. 6.23 Sketch of a coil in two extreme positions along its journey back and forth in the *x* direction.

In the innermost position, the inductance L_E is greatest and in the outermost position it is smallest. The inclusion of the shorting ring minimizes the amount of variation of L_E.

the loudspeaker. The use of a current-source amplifier [16] with motional feedback to provide damping has been proposed in order to minimize this effect. Alternatively, a ferrofluid [17] may be suspended within the magnetic gap. This will effectively conduct heat away from the coil to the pole plate, which acts as a heat sink. Another advantage is that the magnetic fluid reduces the width of the gap to the diameter of the coil wire plus the thickness of the former. A slight disadvantage is that viscosity of the fluid increases mechanical damping and hence reduces Q_{MS}. Ideally, in order to maintain maximum efficiency at resonance, we would prefer all of the damping to be provided electrically so that $Q_{TS} \approx Q_{ES}$ and $Q_{MS} >> Q_{ES}$.

Young's modulus of cone material. At low to mid frequencies, the cone should move as a perfectly rigid piston in which case there is no flexing and the nonlinear stress versus strain relationship should have no effect whatsoever. However, at higher frequencies, vibration modes within the cone will occur and the motion is likely to be nonlinear depending on the amplitude. This can be mitigated by ensuring that either the cone material has sufficient internal damping or that the radial waves are absorbed by a lossy surround. One should also use a crossover which diverts the higher frequencies to another drive unit.

Doppler effect. Suppose that a loudspeaker reproduces two tones simultaneously, one at a sufficiently low frequency to produce significant excursion and the other at a much higher frequency. As the cone moves towards the listener during a positive half-cycle of the low note, the pitch of the high note will be raised by a small amount. Also, as the cone moves away from the listener during a negative half-cycle, the pitch will be lowered. This is the same phenomenon that causes the apparent frequency of a siren to change when an ambulance drives past. Hence, the low note frequency modulates the high note. In practice, the effect is usually minimized through careful choice of crossover frequency [18].

Example 6.3. If the circular gap in the permanent magnet has a radial length of 0.2 cm, a circumference of 8 cm, and an axial length of 1.0 cm, determine the energy stored in the air gap if the flux density is 10,000 gauss.

Solution

$$\text{Volume of air gap} = (0.002)(0.08)(0.01) = 1.6 \times 10^{-6}\ \text{m}^3$$

$$\text{Flux density} = 1\ \text{T}.$$

From books on magnetic devices, we find that the energy stored is

$$W = \frac{B^2 V}{2\mu}$$

where the permeability μ for air is $\mu_0 = 4\pi \times 10^{-7}$ H/m. Hence, the air-gap energy is

$$W = \frac{(1)(1.6 \times 10^{-6})}{(2)(4\pi \times 10^{-7})} = \frac{2}{\pi} = 0.636\ \text{J}$$

Example 6.4. A 5-inch loudspeaker is mounted in one of the two largest sides of a closed box having the dimensions 285 by 189 by 178 mm. Determine and plot the relative power available efficiency and the relative sound pressure level on the principal axis.

Solution. Typical directivity patterns for this loudspeaker are shown in Fig. 4.31. The directivity index on the principal axis as a function of frequency is shown in Fig. 4.32. It is interesting to note that the transition frequency from low directivity to high directivity is about 1 kHz. Since the effective radius of the radiating cone for this loudspeaker is about 0.055 m, ka at this transition frequency is

$$ka = \frac{2\pi fa}{c} = \frac{1000\pi \times 0.13}{344.8} = 1.18$$

or unity, as would be expected from our previous studies. The transition from the circuit of Fig. 6.6(c) [where we assumed that $\omega^2 M_{M1}^2 >> \Re_{MR}^2$ and $\omega^2 L^2 << (R_g + R_E)^2$] to Fig. 6.6(d) also occurs at about $ka = 1$. Now let us model the loudspeaker as a spherical cap in a sphere. From the box dimensions, the equivalent radius R of the equivalent sphere is

$$R = \sqrt[3]{\frac{3(285 \times 189 \times 178)}{4\pi}} = 132 \text{ mm}$$

Since the effective radius a of the cap is 55 mm, the half-angle of the cap is given by $\alpha = \arcsin(55/132) = 25°$. The directivity patterns of a cap of half-angle 30° are shown in Fig. 6.24. Considering the approximate nature of the model, these directivity patterns are remarkably consistent with those shown in Fig. 4.31 for the actual loudspeaker. One advantage of this model is its simplicity since Eq. (12.59) for the directivity pattern is in the form of a fast-converging expansion.

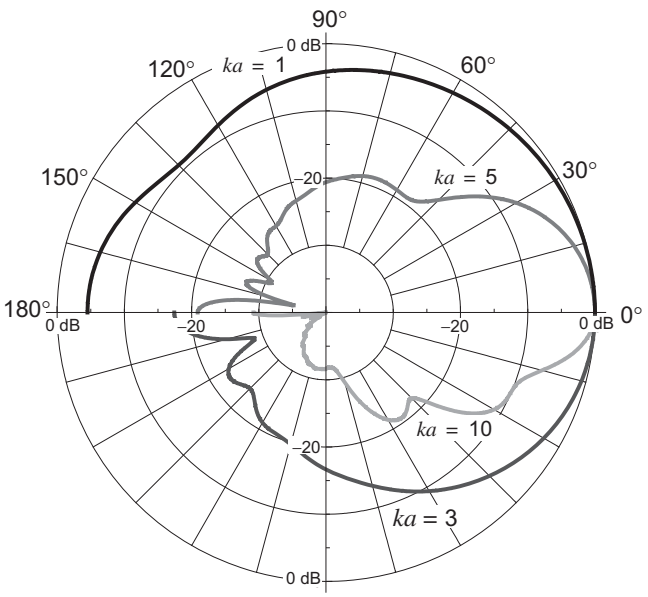

FIG. 6.24 Plots of the directivity patterns of a typical 5-inch-diameter loudspeaker in a closed-box baffle using an oscillating spherical cap in a sphere as a model.

Now, let us determine the sound pressure level on the principal axis of the loudspeaker, using Eqs. (12.58) and (12.61) together with

$$\tilde{u}_c = \frac{Bl}{(R_E + j\omega L_E)j\omega M_{MS}}\tilde{e}_g$$

which is derived from Fig. 6.4(a) assuming that above resonance M_{MS} dominates the loop impedance. Also, let us assume that the amplifier impedance is very low. The results are given by the dashed curve in Fig. 6.25. Above 200 Hz the pressure level starts to rise due to the baffle effect of the enclosure, although the amount of lift is limited by the coil inductance which starts to have effect at around the same point. The cupped shape of the diaphragm helps to maintain a wide directivity pattern at higher frequencies, but the radiated power is falling off, so the sound pressure must also start to fall (unlike with a flat piston where the concentration of sound on its axis maintains a level output). The fact that the model uses a convex dome as opposed to a concave cone will introduce errors but a quick comparison of Fig. 12.28 with Fig. 12.32 for a convex and a concave dome respectively shows that the trends are broadly similar. Hence we see a second-order or 12 dB/octave high-frequency roll-off due to the compounded effect of the diaphragm inertia and coil inductance. Also at higher frequencies, cone resonances occur, as we said before, and the typical response curve of Fig. 6.14 is obtained.

In order to calculate the efficiency, let us assume that it is mounted in an infinite baffle and that one-half the power is radiated to each side.

The efficiency, *from one side of the loudspeaker*, is given by Eq. (6.57) divided by 2, where for the frequency range well above resonance we have used the approximations

$$Z_{MT} \approx j\omega M_{MS} \text{ and } Z_E \approx R_E + j\omega L_E.$$

From this we obtain the solid curve of Fig. 6.25*a*. It is seen that, above $f = 1000$ Hz, the efficiency drops off.

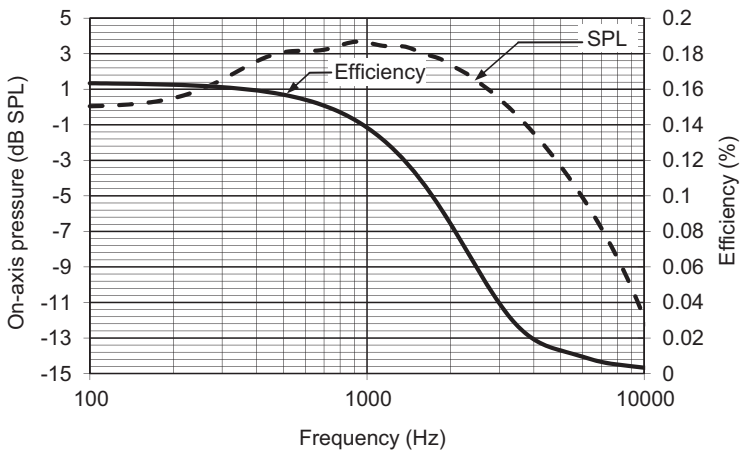

FIG. 6.25 Graphs of the computed efficiency and sound pressure level measured on the principal axis of a typical 5-inch-diameter loudspeaker in a closed-box baffle.

$R_E = 6.6\ \Omega$, $L_E = 0.5$ mH, $Bl = 4.5$ Tm, and $M_{MS} = 9.6$ g. The reference level is chosen arbitrarily.

References

[1] Villchur EM. Problems of bass reproduction in loudspeakers. J. Audio Eng. Soc. 1957;5(3):122–6.

[2] For supplemental reading, the student will find the following publication valuable. In: Borwick J, editor. Loudspeaker and Headphone Handbook. 3rd ed. Oxford: Focal Press; 2001.

[3] Rice CW, Kellogg EW. Notes on the development of a new type of hornless loudspeaker. J Audio Eng Soc 1982;30(7/8):512–21. Abridgment of paper presented at the Spring Convention of the A.I.E.E., St. Louis, April 13-17, 1925. U.S. Patent No. 1,795,214. Previous patents for moving-coil transducers were granted to Ernest Siemens in 1874 (US patent no. 149797) and Sir Oliver Lodge in 1898 (British patent no. 9712).

[4] W. Klippel, Prediction of Speaker Performance at High Amplitudes, in the 111th AES Convention, 2001, paper no. 5418.

[5] Small RH. Direct Radiator Loudspeaker System Analysis. J Audio Eng Soc 1972;20(5):383–95.

[6] Klippel W. Assessment of voice-coil peak displacement X_{max}. J Audio Eng Soc 2003;51(5):307–23.

[7] See IEC 60268–5, ed. 3.1, Sound system equipment - Part 5: Loudspeakers, available from http://webstore.iec.ch/. For example, for a nominal 8-in (200 mm) diameter loadspeaker, the baffle size would be 1.65 m long by 1.35 m wide, with the loadspeaker offset from the center by 22.5 cm lengthways and 15 cm widthways.

[8] http://www.electronenergy.com/

[9] Mellow TJ, Kärkkäinen LM. On the sound field of a shallow spherical shell in an infinite baffle. J Acoust Soc Am 2007;121(6):3527–41.

[10] Frankort FJM. Vibration patterns and radiation behavior of loudspeaker cones. J Audio Eng Soc 1978;26(9):609–22.

[11] Lerch R, Kaltenbacher M, Meiler M. Virtual prototyping of electrodynamic loudspeakers by utilizing a finite element model. J Acoust Soc Am 2008;123:3643.

[12] Corrington MS. Amplitude and phase measurements on loudspeaker cones. Proc. IRE 1951;39:1021–6.

[13] A tone burst is a wave-train pulse that contains a number of waves of a certain frequency.

[14] Klippel W. Tutorial: Loudspeaker nonlinearities – causes, parameters, symptoms. J Audio Eng Soc 2006;54(10):907–39.

[15] S. Hutt, Loudspeaker spider linearity, in the 108th AES Convention, 2000, paper no. 5159.

[16] Mills PG, Hawksford MJ. Distortion reduction in moving-coil loudspeaker systems using current-drive technology. J Audio Eng Soc 1989;37(3):129–48.

[17] Bottenberg W, Melillo L, Raj K. The dependence of loudspeaker design parameters on the properties of magnetic fluids. J Audio Eng Soc 1980;28(1/2):17–24.

[18] Allison R, Villchur E. The audibility of doppler distortion in loudspeakers, in the 70th AES Convention, 1981, paper no. 1844.